ChemComm

FEATURE ARTICLE

The Use of Mixed-Metal Single Source Precursors for the Synthesis of Complex Metal Oxides

Received 00th November 2019,
Accepted 00th December 2019

DOI: 10.1039/x0xx00000x

Haijiao Lu,[a,b] Dominic S. Wright,[*b] Sebastian D. Pike[*b,c]

Complex metal oxides, defined as metal oxide materials with multiple metals, phases or including dopants, are used in a huge variety of modern applications ranging from photocatalysis, transparent conductive materials, supercapacitors and battery components. In this feature article, the use of mixed-metal single source precursors to synthesise complex metal oxides is explored. The structures and decomposition/reaction pathways of various precursors including mixed-metal alkoxides, complexes with chelating ligands, clusters, polyoxometallates, and metal-organic frameworks are discussed. The advantages and opportunities of using a single source precursor strategy are investigated and highlighted.

Haijiao Lu completed her PhD at Tianjin University (China) in 2019. She was a PhD student at Tianjin University under the supervision of both Prof. Jingkang Wang and Prof. Hongxun Hao since 2014 and a visiting student supervised by both Prof. Dominic S. Wright and Dr. Sebastian D. Pike at the University of Cambridge from 2017 to 2019. She currently works at the Australian National University as a post-doctoral fellow in the research group of Associate Prof. Zongyou Yin from August 2019. She is interested in the synthesis of metal oxide materials by the single-source precursor method for applications in photocatalysis, such as photocatalytic water splitting and CO_2 reduction.

Dominic S. Wright obtained a first in pure and applied chemistry at Strathclyde University (1982-1986) before moving to Cambridge in 1989, where he undertook Ph.D. study under the supervision of the late Ron Snaith (1986-1989). He gained a college research fellowship at Gonville and Caius College Cambridge (1989-1991), before becoming a lecturer in the inorganic section (1991- 2002). He was promoted to reader in 2002. Wright has published over 330 papers on diverse aspects of main group and transition metal chemistry. He was the recipient of the 1993 Royal Society Meldola Medal and the 2012 RSC Main Group Chemistry Award.

Sebastian D. Pike completed his D.Phil at the University of Oxford in 2014 under the supervision of Prof. Andrew Weller. He then studied at Imperial College London as a Post-Doctoral Research Associate in the research groups of Prof. Charlotte Williams and Prof. Milo Shaffer. In 2016 he was awarded a Herchel Smith Research Fellowship at the University of Cambridge to begin his own independent research. In 2019 Seb was awarded a Royal Society University Research Fellowship and recently moved to the University of Warwick. His research interests sit at the interface between molecular and materials chemistry, with a focus on studying well defined metal-oxo clusters as photoactive analogues of bulk semiconductors and using mixed-metal molecular systems as single source precursors for functional materials such as $BiVO_4$.

1. Introduction

Metal oxides possess a vast variety of compositions, structures and properties and are one of the largest and most applicable classes of solid materials. Metal oxides have significant and diverse applications, they may be used in solar cells,[1] photocatalysts,[2] batteries,[3] transistors,[4] ferroelectric and

[a.] School of Chemical Engineering and Technology, Tianjin University, Tianjin 300072, China.
[b.] Department of Chemistry, University of Cambridge, Lensfield Road, Cambridge, CB2 1EW, United Kingdom
[c.] Department of Chemistry, University of Warwick, Coventry, CV4 7EQ.
Corresponding authors: dsw1000@cam.ac.uk, sp842@cam.ac.uk.

multiferroic materials,[5] supercapacitors,[6] superconductors,[7] luminescent materials[8] and gas sensors.[9] The properties of metal oxides can be enhanced by introducing hetero-metals either as stoichiometric components or as dopants. This increases the complexity of synthesis. In this article we explore the use of molecular single source precursors (SSPs) to access metal oxide materials with at least two incorporated metals. We define this broad group of materials as complex metal oxides (CMOs) which include mixed-metal oxides ($A_xB_yO_z$), hetero-metal doped metal oxides ($B:A_xO_y$) or composite metal oxides with a mixture of oxide phases (A_wO_x/B_yO_z). Today, many types of mixed-metal oxides are accessible from SSPs including perovskites (ABO_3),[10-16] pyrochlores ($A_2B_2O_7$),[17] spinels (AB_2O_4),[18-25] metal vanadates $[M_x(VO_4)_y]$,[26, 27] feldspars ($MAl_2Si_2O_8$)[28] and Aurivilius phases $(Bi_2O_2)(A_{n-1}B_nO_{3n+1})$.[29]

Traditional Synthesis of Complex Metal Oxides

The synthesis of CMOs is often challenging, due to difficulties with controlling the exact stoichiometry, structure and homogeneity of the final species.[11, 12, 15, 30] Such challenges are not helped by the harsh conditions often required for traditional 'ceramic' solid-state synthesis.[30, 31] Conventional ceramic routes include solid-state reactions using oxide, carbonate, or nitrate precursors, often requiring high temperature processing, particularly if highly-crystalline products are required.[32] These approaches may give poor control over stoichiometry and phase purity.[12, 33, 34] High temperature methods can drive phase separation and/or may only access thermodynamic products,[15] and volatile components can also be released altering the designed stoichiometries.[35] High temperatures also dictate the crystallinity, particle size and porosity of the produced materials, reducing opportunities to design specific attributes for applications. For these reasons, 'soft chemistry' techniques using a bottom up molecular approach have played a major role in simplifying CMO synthesis, improving efficiency and enabling access to new material properties (i.e. kinetically controlled products).[10, 36] Many CMOs can be prepared from multi-source precursors (i.e. a mixture of homometallic molecular precursors), however, this approach, whilst simple, can lead to difficulties if the multiple precursors have different physical properties such solubility or reactivity. If employing a solution based deposition process (e.g. drop-casting) different solubilities could result in phase separation during a drying step such that the multi-source precursors crystallise separately leading to an inhomogeneous film before calcination.[37, 38] During hydrolytic reaction routes, such as sol-gel processes, differing reactivity of single-metal species can lead to phase-separation and is likely to lead to an imperfectly mixed product.[11]

Opportunities Using Mixed-Metal Precursors

The use of mixed-metal (heterometallic) complexes or frameworks, which contain more than one metal, as SSPs provides alternative synthetic routes to access CMOs.[11, 39, 40] Using an SSP has been reported to display advantages such as simplifying material synthesis;[26, 27] access to unusual or otherwise inaccessible products;[12, 30, 41] or materials with enhanced performance.[42-44] By incorporating all of the required metals into one precursor, the stoichiometry is defined at the molecular level. CMOs may then be obtained after reconstruction of the molecular connectivity, and elimination of supporting organic groups in the SSPs, sometimes requiring hydrolysis. Pre-existing bonds in the precursor molecules, especially M–O connections, have been postulated to lower the nucleation barrier to form solid-phase materials and thus may allow access to CMOs at lower temperatures.[30] Regardless of any preformed M–O bonding, the mixed-metal precursors at

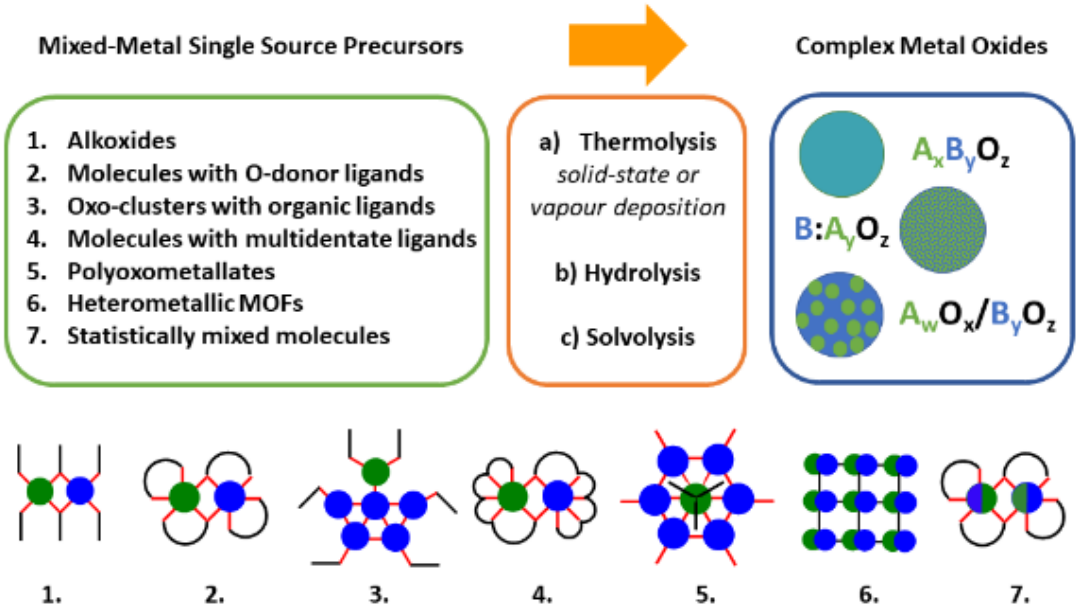

Fig. 1 Routes to convert a mixed-metal single-source precursor into the different varieties of complex metal oxide.

least reduce the diffusion distances required to assemble the CMO structure.[32] By using lower synthesis temperatures, CMOs can be produced with small particle sizes and large surface areas,[30, 45] or deposited onto more delicate substrates. The large amount of heat released from the decomposition of organic molecules can also facilitate the crystallisation of pure-phased oxides at relatively low reaction temperatures, enabling formation of high surface-area nanoporous structures otherwise unobtainable at higher temperatures.[37] Compared to (multi-source) single-metal molecular precursors, mixed-metal complexes often ensure a much more accurate stoichiometry and better homogeneity of target metals as the component elements are precisely distributed within the molecular precursor.[30, 43, 44, 46] An SSP may contain a perfect inter-metal stoichiometry for conversion to a pure phase mixed-metal oxide, or alternatively, can contain a mixture of metals which transform into two or more (interpenetrated) oxide phases (previously defined by Veith as a type 3 SSP).[11, 47, 48]

Mixed-metal SSP compounds are often soluble in organic solvents (and sometimes water), allowing convenient routes to fabricate thin films of CMOs, by straightforward techniques (such as drop-casting and spin-coating),[26, 27, 35, 49, 50] spray pyrolysis,[51] sol-gel processes[11, 15, 52] or (aerosol-assisted) CVD.[53] The use of a single precursor under mild reaction conditions also simplifies CMO synthesis for applications that demand excellent material homogeneity across a large scale.[4, 26, 42, 54]

Of course, the advantages of using an SSP may be offset by the challenges and costs of prepraring a specifically designed molecular precursor, which is an important consideration for practical use.

In this feature article, we summarize the main types of mixed-metal species that have been reported as SSPs for the synthesis of CMOs (**Fig. 1**), varying from the well documented mixed-metal alkoxides to newer approaches such as using metal-organic-frameworks as precursors, or using multi-metallic metal-oxo cluster SSPs – aspects of which our research group have been recently exploring.

2. General Methods to Access CMOs from Single-Source Molecular Precursors

2.1 Thermal decomposition

2.1.1 Solid-State Thermolysis

Thermal decomposition of a mixed-metal SSP in the solid phase is a straightforward way to prepare CMOs. The precursors decompose at elevated temperatures, with loss or decomposition of any organic components to form CMOs. Control of the heating rate is important to direct decomposition in preference to melting/vaporisation of the molecular species which can occur upon rapid heating.[10] The advantage of a solid-phase transition is the retention of the elemental composition, defined by the molecular precursor, with only loss of volatile decomposition products – allowing excellent stoichiometric control of the inter-metal ratio in the CMO products.

SSPs may be designed to exhibit good solubility, allowing for straightforward solution deposition techniques such as drop, spin or spray coating to generate thin (microcrystalline) films of the SSP, ready for thermal decomposition to a thin film. The chemistry involved with deposition and drying of precursors may be remarkably complex and can be important with respect to the material that forms after subsequent calcination.[35]

Modern techniques allow for *in-situ* characterisation of the decomposition and calcination process by temperature-controlled powder X-ray diffraction studies.[55] The maximum heating temperature (and also the rate of temperature increase) has been shown to affect the products of these reactions.[30, 55-58] Many examples state the ability of SSPs to decompose and crystallise into CMOs at much lower temperatures than in traditional solid-state ceramic methods.[11, 12, 18, 23, 34, 41, 42, 54, 56, 59]

Decomposition of metal-organic species requires the release of gaseous organic decomposition products (and possibly solvent molecules), and the release of these gases may influence the particle size and porosity of the produced oxide. Higher organic content in precursors allows for greater porosity and smaller particle sizes in their decomposition products, attributed to greater gas escape during thermolysis.[55, 56, 60] Care should be taken in choosing the maximum heating temperature during annealing, as volatile metal compounds (e.g. Li_2O or PbO) can also be lost, negating the carefully constructed intermetal ratio in the SSP.[61]

The combustible content of an SSP is also important for internal heating of the sample and aiding crystallisation, however, too much organic content can lead to carbon impurities in the final product and/or can lead to reduction of metals (such as Bi(III) to metallic Bi).[55]

2.1.2 Chemical Vapour Deposition

Typically, during the (Metal-Organic) Chemical Vapour Deposition (CVD) process, liquid precursors are volatilised at an intermediate temperature (<200 °C), before rapid decomposition upon a high temperature substrate leaving a thin film deposit of CMO product.[5, 10, 40, 62-65] Using a mixture of mono-metallic precursors can lead to difficulties due to the different physical properties, stabilities and decomposition characteristics of the multiple components.[5, 39, 54, 66] If very high temperatures are used to overcome these difficulties, this may lead to an increase in lattice defects in the deposited film.[54] It may be possible to simplify a CVD process by employing a single precursor molecule rather than a mixture of species with differing volatilities. However, it is important that any SSPs remain stable during evaporation to maintain the singular nature of the precursor.[67-69]

Carbon impurities can be detrimental for applications of CMOs and judicious choice of ligands is required during CVD processes to ensure no carbon is retained.[39]

Aerosol assisted CVD (AACVD) reduces the requirement for highly volatile precursors and is a useful method for utilising mixed-metal SSPs,[63] for example in the formation of thin films of $FeSnO_x$ from Fe-Sn SSPs[70] or mixtures of $CdTiO_3/TiO_2$ from Cd-Ti_2 SSPs.[71]

2.2 Hydrolysis

When basic metal-organic compounds (e.g. organometallics, metal amides or metal alkoxides) are exposed to water molecules, either within solution or when exposed to ambient air, they are susceptible to hydrolysis and polycondensation by elimination of small or volatile molecules (e.g. alkanes, arenes, amines or alcohols).[72] During hydrolysis, water molecules provide H^+ for removal of ligands and O^{2-} for formation of metal oxides. Sol-gel techniques are commonly applied to use this reactivity to generate oxide materials. In sol-gel routes, hydrolysis generates small metal oxide particles, which grow and interlink together via condensation to form a gel of nanostructures protected by residual ligands/hydroxides.[38] Additional multidentate ligands or polymers may be added to improve the homogeneity of the gel phase. This amorphous gel then requires calcination to form a bulk oxide phase,[10, 73] potentially with access to different product compositions when heated to different temperatures.[78] Sol-gel routes are favoured for their simplicity and ability to influence the final particle morphology, although they may require careful control of multiple parameters (e.g. temperature, solvent, concentration) to ensure reproducibility.[74] In aqueous reactions, water plays a dual role of both ligand and solvent, and so it can be difficult to control the rate and degree of hydrolysis, condensation, and aggregation, in turn causing difficulties in controlling the crystallinity, morphology, and reproducibility of the CMOs produced.[74]

Whilst SSPs begin as mixed-metal species, solution-based hydrolysis processes do not guarantee that the intermediate species during a hydrolysis reaction retain the inter-metal ratio, in fact, it is generally considered that in solution-phase reactions, where molecules can rapidly equilibrate, there is no 'memory' of the previous step, as indicated by the partial hydrolysis of mixed-metal alkoxide precursors.[10, 68, 75] It is possible that the introduction of covalently bonded bridging oxo groups may introduce an energy barrier to rearrangement, but may still ultimately require bond redistribution in order to form the final oxide product.[23] Therefore, using SSPs in sol-gel syntheses may not lead to homogeneously mixed oxide products, and instead may preferentially generate biphasic composites.[36, 76, 77] One possible solution is to connect metals with a bifunctional ligand so that they retain a close proximity despite differing rates of hydrolysis.[46]

2.3 Solvolysis

Although aqueous sol-gel routes are commonly used for the synthesis of metal oxides, non-aqueous reaction routes using organic solvents have also been developed and can be applied to gain control over the rate of condensation and to obtain metal oxides with high crystallinity and narrow size distribution at low temperatures.[79, 80] In most non-aqueous processes, the oxygen for metal oxides is derived from the O-containing solvent,[34] or O-containing components in the precursors.[43] Solvolysis condensation reactions involve the formation of M–O–M bonds and elimination of an ester, ether or alkyl halide; C–C bond formation; or the aldol or ketimine condensation reactions (**Fig. 2**), depending on the structures of both the precursor and the solvent (examples are discussed in section 3.2 and 3.8).[43, 79] The solvent molecules play important roles in the condensation mechanisms, but they also have significant effects on the size, shape, morphology and even surface composition of the metal oxides produced.[46, 74, 81]

3. Mixed-metal SSPs for synthesis of CMOs

3.1 Synthetic strategies

Various strategies can be used to form mixed-metal precursors (**Fig. 3**). Initial studies focused on building mixed metal alkoxides followed by derivations of these systems that incorporate chelating O-donor ligands. Structures based on simple adducts of mono-metallic components can be susceptible to segregation, and thus a more robust strategy may be used to build a covalent bridge between metals. Oxo bridged M–O–M' structures can be prepared by the reaction of (basic) organometallic complexes with (acidic) metal hydroxides,[82]

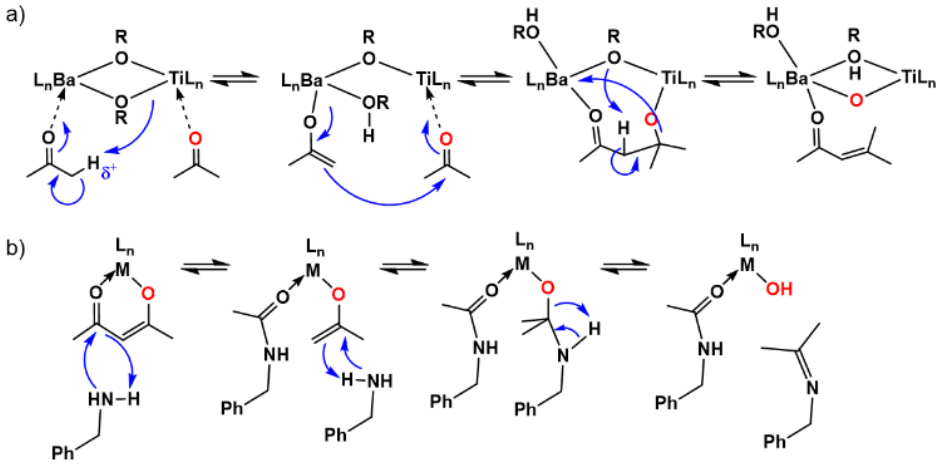

Fig. 2 Solvothermal mechanisms introducing metal oxo or metal hydroxide functionalities (O shown in red) leading ultimately to the condensation of a metal oxide. (a) Aldol condensation in the process of forming $BaTiO_3$ from $BaTiO(O^iPr)_4$ in dry acetone; (b) General process for ketimine condensation from an acetylacetonate ligand and benzylamine.

likewise organometallic reagents can react with pendant acidic OH groups on multidentate ligands.[13, 14, 19, 83-86] Bifunctional (ambidentante) linker ligands with differing coordination sites can allow for stepwise attachment of two different metals (one at either site[36]) as shown in Zn-Ti SSP ($\{Zn(POBC)_2Ti(O^iPr)_3\}_2$) (POBC-H = *p*-carboxybenzaldehyde oxime).[46, 87] Similarly, utilising the affinity of benzene rings to coordinate to the $Cr(CO)_3$ fragment allows the formation of Zn-Cr precursors $[MeZnOCH_2PhCr(CO)_3]_4$ and $[MeZnOCH(PhCr(CO)_3)_2]_2$, useful for $ZnCr_2O_4$ synthesis.[18] The ferrocene unit is also a convenient group for including Fe into a molecule, examples include Fe-Sn precursors $(C_5H_5)Fe(C_5H_4)C_6H_4CO_2SnR_3$.[70] Inclusion of extra metals within counterions is another versatile approach, which creates a perfect distribution of the metals when crystallised in an ionic lattice and can allow a variety of secondary/tertiary metals to be incorporated into isostructural compounds.[26, 27] Rare examples of mixed-metal precursors may even incorporate direct M–M' bonding, such as the polymeric $Cp(CO)_2Fe–BiCl_2$ compound, useful for synthesis of the photocatalyst $BiFeO_3$ using AACVD methods.[88, 89]

Another synthetic strategy is to incorporate metals in a statistical mixture into a well-defined structural motif, for example the partial transmetallation of a monometallic cluster precursor to introduce a secondary metal.[90] Here, we define this type of precursors as 'imprecise SSPs' and discuss them separately at the end of this section.

Heterobimetallic SSPs can also be produced *in-situ* by a direct combination of monometallic reagents during CMO synthesis. Care should be taken that a true mixed-metal SSP is forming rather than a mixture of precursors. However, this approach does allow for a straightforward synthetic process.

It is generally considered that excluding halide ligands from precursors is advantageous for the formation of clean oxide materials, although several examples have now shown that post-calcination washing steps can remove any halide contaminants (which are often highly soluble) from the desired oxide phase.[12, 26, 83, 89, 91, 92]

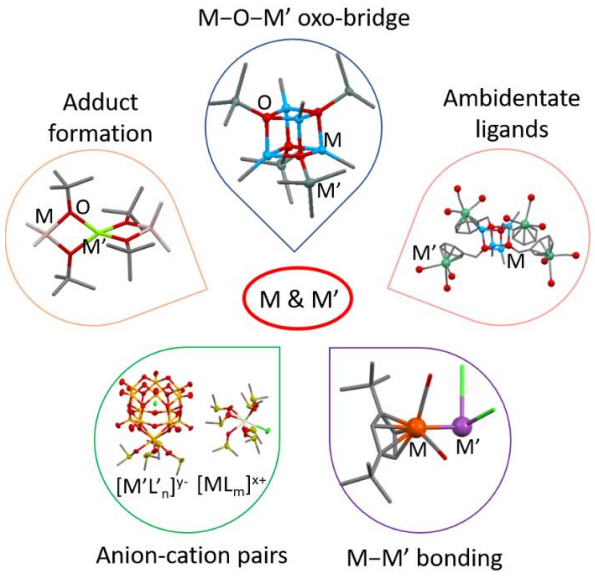

Fig. 3 A variety of options for creating heterometallic compounds.

Whilst it is difficult to straightforwardly collect the multitude of different SSPs into set categories, in the following sections we have attempted to group the literature examples into five major groupings of molecular SSPs, plus a group of extended framework precursors and a final section upon statistically mixed mixed-metal species.

3.2 Mixed-metal alkoxides

Mixed-metal alkoxides are a group of compounds in which different metals are bridged by alkoxy groups. This family of compounds dates back to 1929 when $Na[Al(OR)_4]$ was first synthesised.[64, 93] Generally, they are formed by Lewis acid – Lewis base interactions by simply mixing homometallic alkoxides, although in some cases a metathesis reaction utilising metal chlorides and a group 1 metal alkoxide has also proven useful.[77, 78, 94, 95] Rapid exchange of alkoxide ligands may be observable by variable temperature nuclear magnetic resonance (NMR) spectroscopy.[5] A huge number of mixed-metal alkoxides have been reported and those with the same oxidation states and intermetal ratios tend to display analogous and predictable structures.[12, 72, 96] However, synthesis of these compounds can be sensitive to experimental conditions, including solvent or the nature of the alkoxide group, and thus precursors with differing intermetal ratios may be obtainable, e.g. $PbZr(O^tBu)_6$ *vs.* $Pb_2Zr_4(O^iPr)_{20}$.[64] Difficulties can arise when the monometallic alkoxides exist as insoluble polymers, as commonly found for $M^{II}(OR)_2$ compounds. Utilising alkoxides with pendant donor groups (e.g. $^-OC_2H_4OMe$ or $^-OC_2H_4NMe_2$) can enhance stability and solubility and access different precursors.[20] Another tactic is to use alkoxide ligands with α-substituents that block oligomerisation, this can be useful for designing volatile precursors for CVD processes.[39]

On some occasions, mixing different metal alkoxides which exist with identical molecular geometries can lead to a statistical mixture of the metals within the alkoxide structures. This is referred as isomorphous substitution, and can still provide homogenization at the molecular level (see 'imprecise' SSPs in section 3.8).[96]

Although bimetallic alkoxides are common, the formation of trimetallic alkoxides is challenging; limited examples have been fabricated including $[Cd(O^iPr)_3]M(M'_2(O^iPr)_9]_2$ (M = Ba, Sr; M' = Sn, Ti, Zr, Hf),[97, 98] and $[Al(O^iPr)_4][(HO^iPr)BaM_2(O^iPr)_9]$ (M = Hf or Zr)[99] (**Fig. 4**) which have been synthesised through stepwise construction under kinetic control.

Whilst mixed-metal alkoxides can act as useful synthons to generate further mixed-metal compounds, they themselves often suffer from poor stability and/or may be in equilibrium with their mono-metallic components, limiting their direct use as SSPs.[52, 100] Donor solvents may also disrupt the adduct coordination, resulting in the separation of homometallic alkoxides with segregation of the metals.[101]

Despite their limitations, there are many examples of mixed-metal alkoxides producing useful CMOs. Early studies of SSPs in sol-gel chemistry developed precursors for the useful perovskite $BaTiO_3$ which can be used in capacitors or

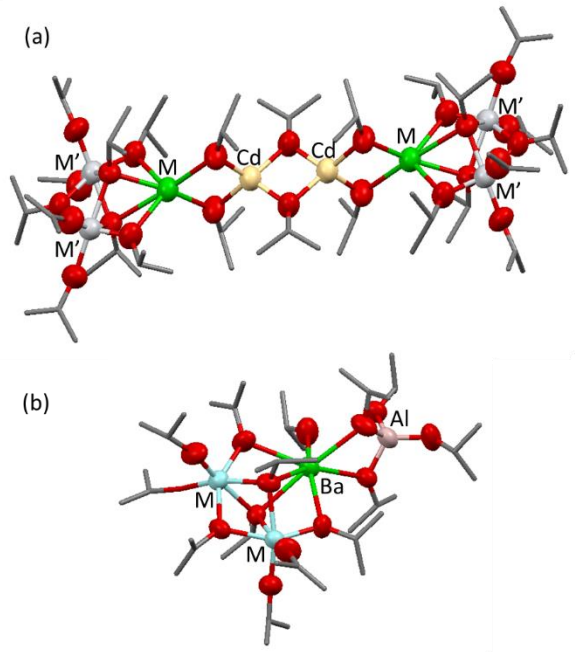

Fig. 4 Solid-state structures of (a) $[Cd(O^iPr)_3]M(M'_2(O^iPr)_9]_2$ (M = Ba, Sr; M' = Sn, Ti, Zr, Hf) and (b) $[Al(O^iPr)_4][(HO^iPr)Ba\{M_2(O^iPr)_9]$ (M=Hf or Zr).

transducers.[11, 52] This work culminated in the use of mixed-metal alkoxides, such as $BaTiO(O^nBu)_4(^nBuOH)$, in industrial processes, to prepare $BaTiO_3$ films. The related $BaTiO(O^iPr)_4{\cdot}^7/_8{}^iPrOH$ has also been shown to produce $BaTiO_3$ by non-aqueous routes. This Lewis acidic SSP reacts with dry acetone (or cyclohexanone) via an aldol condensation at room temperature, allowing very low temperature synthesis of $BaTiO_3$,[34] and avoids multigrain particles which affect the dielectric properties of the perovskite that can occur from high temperature ceramic synthesis (**Fig. 2a**). However, as with any solution sol-gel process, the stoichiometry of the SSP may not be accurately reflected in the CMO, and in this case a minor excess (4% extra) of Ti is found, indicating that solution rearrangements may allow some metal segregation.

Further examples of the use of mixed-metal alkoxides as SSPs that produce pure CMO products and avoid impurities are $[YFe(O^iPr)_6(^iPrOH)]_2$ and $Mg_2Ti_2(OEt)_{12}(EtOH)_4$. $[YFe(O^iPr)_6(^iPrOH)]_2$ is converted into the weak ferromagnetic perovskite $YFeO_3$ (which as a kinetic product, is difficult to prepare by other routes) by low temperature sol-gel hydrolysis followed by annealing (**Fig. 5a**). This process avoids the formation of Fe_3O_4 or $Y_3Fe_5O_{12}$ impurities which are commonly obtained when using other methods.[15] $Mg_2Ti_2(OEt)_{12}(EtOH)_4$ decomposes in the solid phase to produce $MgTiO_3$ at 900 °C without common contaminant phases like $MgTi_2O_5$ or Mg_2TiO_4. $MgTiO_3$ is employed in capacitors or resonators in communication devices, however, producing phase-pure $MgTiO_3$ is recognized to be difficult by previous studies, for instance, a solid-state reaction, which requires a sintering temperature of over 1400 °C, gives final materials that contain a certain amount of $MgTi_2O_5$.[12]

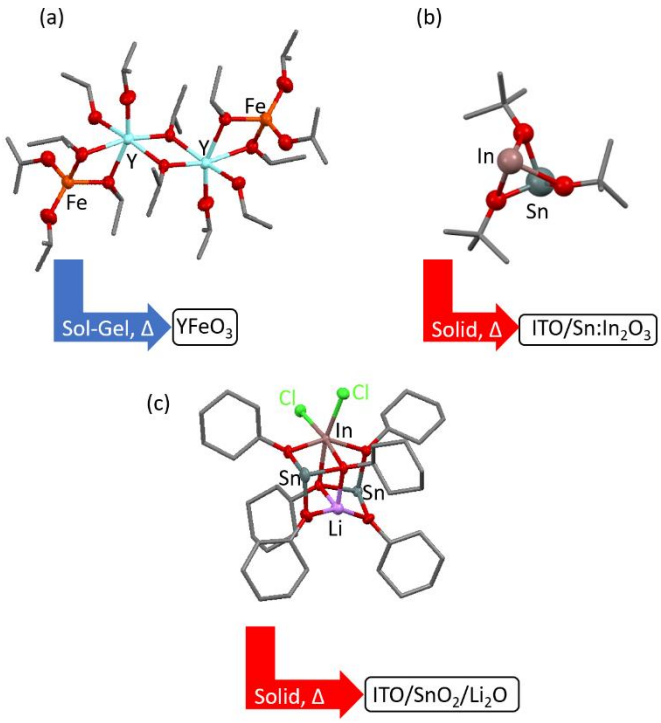

Fig. 5 Heterometallic alkoxide SSPs (a) $[YFe(O^iPr)_6(^iPrOH)]_2$ (b) $In^ISn^{II}(O^tBu)_3$ (c) $Cl_2In\{LiSn^{II}_2(OCy)_6\}$ and their decomposition products.

Another interesting alkoxide precursor is the molecule $In^ISn^{II}(O^tBu)_3$ which can be used as a precursor for Sn rich (indium tin oxide) ITO (**Fig. 5b**).[42] ITO is an important transparent conductor with a low percentage of Sn (~5-15 mol%), but as indium is expensive there is interest in generating equally conductive and transparent materials with a lesser indium content. $InSn(O^tBu)_3$ can be thermally decomposed into a solid solution of crystalline particles of ITO in an amorphous tin rich indium oxide matrix. The use of the SSP allows high Sn content whilst maintaining excellent transparent conductivity (resistivity 4.1 $x10^{-3}$ Ωcm). In contrast, conventional routes to ITO are restricted to <15 mol% Sn content otherwise $In_4Sn_3O_{12}$ formation or In_2O_3/SnO_2 segregation is observed. Furthermore, $InSn(O^tBu)_3$ combined with block-co-polymers can be used to prepare mesoporous Sn rich ITO. As crystallisation of ITO is not essential for the required properties, low formation temperatures can be used allowing for retention of a high surface area.[102] Trimetallic $X_2In^{III}\{LiSn^{II}_2(OCy)_6\}$ (X = Cl or Br) utilises indium in its more stable +3 oxidation state with an even lower metal percentage of indium, and thermal degradation led to $ITO/SnO_2/Li_2O$ and produced thin film field-effect transistors at low temperatures which showed good performance (with saturation electron mobilities of up to 6.36 $x10^{-1}$ $cm^2V^{-1}s$) especially considering the low In content (**Fig. 5c**).[50]

Similarly to metal alkoxides, organometallic precursors are often moisture sensitive, however, alkyl groups have a lesser tendency to act as a bridging ligand than alkoxides, which reduces the tendency of a complex to dimerize and hence may improve volatility.[83] $Mg[(\mu\text{-}O^tBu)_2AlMe_2]_2$ is an example of a

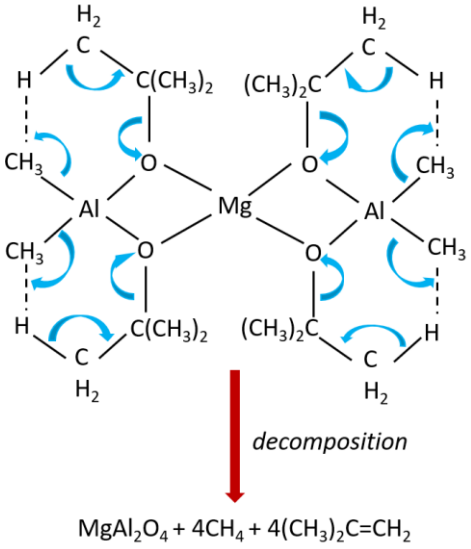

Fig. 6 Schematic illustration of the pathway of the $Mg[(\mu\text{-}O^tBu)_2AlMe_2]_2$ SSP to form $MgAl_2O_4$ via elimination of methane and Me_2CCH_2.

mixed alkoxide/alkyl mixed-metal SSP (**Fig. 6**).[54] The high volatility of this complex makes it an ideal candidate for CVD processes. The SSP transforms into $MgAl_2O_4$ films at merely 400 °C, with ideal stoichiometry, no carbon impurities, and excellent homogeneity confirmed by Auger depth profiling.[54] In contrast, high temperatures (≥1000 °C) are often required to deposit $MgAl_2O_4$ films by CVD when using separate Mg and Al precursors, this can result in unacceptable deviation of the stoichiometry, excessive tensile stress and lattice defects. The clean, controlled decomposition of $Mg[(\mu\text{-}O^tBu)_2AlMe_2]_2$ is partially attributed to its smooth decomposition via charge redistribution reactions such as that proposed in **Fig. 6** (e.g. the hydrocarbons CH_4 and $CH_2{=}CMe_2$ are eliminated as gases as the only by-products).[11, 45]

Replacing alkoxide or amido groups with tin containing $^-OSnR_3$ or $^-N(SnR_3)_2$ moieties allows direct formation of heterobimetallic complexes,[103] an example being the $[R_3SnOZnR']_4$ (R = Me, Ph, R'=Me, Et, ^{t}Bu) cubanes which can be used for the production of Sn doped ZnO and/or Zn_2SnO_4 tested as field-effect or thin-film transistors (**Fig. 7a**).[104, 105] It should be noted that thermal degradation leads to loss of Sn content when R = Me, due to the volatility of the $SnMe_3$ fragment above 115 °C, but Sn loss is almost entirely overcome by replacement of Me by Ph, albeit with a slight increase in carbon impurities in the product.[104] The Sn content of the final product can also be adjusted by mixing in monometallic Zn cubane precursors. As an alternative to alkoxides, siloxide groups can introduce silicon into the precursors, for example, allowing direct formation of high-melting point $MAl_2Si_2O_8$ feldspar ceramics (useful in aerospace applications) from $[M\{(\mu\text{-ddbfo})_2Al(OSiR_3)_2\}_2]$ (M=Ba, Sr, ddbfoH=2,3-dihydro-2,2-dimethylbenzofuran-7-ol) (**Fig. 7b**).[28]

3.3 Mixed-metal complexes with other O-donor ligands

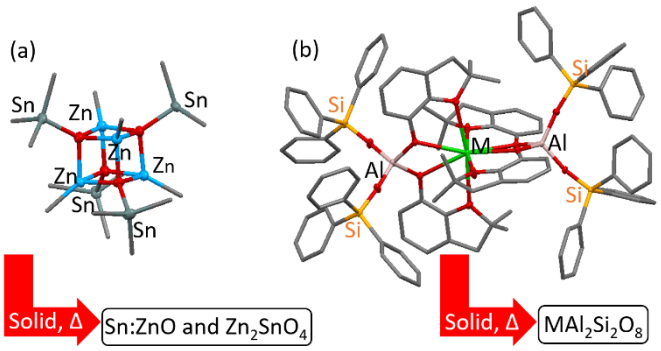

Fig. 7 Solid state structures of heterometallic SSPs (a) $[(CH_3)_3SnOZnCH_3]_4$ and (b) $[M\{(\mu\text{-ddbfo})_2Al(OSiR_3)_2\}_2]$ (M = Ba, Sr) and their decomposition products.

Introduction of further oxygen donor ligands, including bidentate ligands, such as carboxylates[64, 106] and β-diketonates,[16, 21, 57, 61, 76, 107, 108] opens up further possibilities for mixed-metal complexes including main group or late transition elements, which otherwise can be difficult to form or are inaccessible as simple mixed-metal alkoxides.[72, 101] Combining multiple ligands and metals together can lead to a wide variety of mixed metal/mixed ligand complexes useful as SSPs.[5] The use of a mixture of ligands with different Lewis bacisities can help promote heterobimetallic complexation.[57, 109] In general, these ligated complexes tend to exhibit better solubility in common organic solvents and have a greater stability against hydrolysis compared to simple mixed-metal alkoxides, making them more useful precursors for the formation of CMOs.[52] Although it should be noted that the use of polar coordinating solvents can lead to dissociation into solvent supported homometallic precursors.[64] Importantly, the thermal decomposition of carboxylate and acetylacetonate ($acac^-$) ligands is often shown to progress at similar temperatures to alkoxides, allowing for smooth thermal decomposition pathways of heteroleptic complexes.[76] Large bulky ligands, such as 2,3-dihydro-2,2-dimethylbenzofuran-7-ol, may require a long thermolysis process to completely remove organic contaminants from the desired oxide products.[19, 84]

Kessler and co-workers have designed a wide range of similarly structured mixed-metal precursors, based on the requirements of metal coordination number;[96] especially those based on a combination of M^{5+} and M^{2+} metals within the common structures $M^{(V)}_2M^{(II)}_2(L)_2(OR)_{12}$ or M^{4+} and M^{2+} with structures $M^{(IV)}_2M^{(II)}_2(L)_4(OR)_8$, where L = a bidentate β-diketonate ligand.[67, 100, 110, 111]

Difficulties can arise if a heterobimetallic complex is susceptible to thermal deconstruction, for example, $Ba_2Ti_2(thd)_4(OEt)_8(EtOH)_2$ (thd = tetramethylheptanedionate) and $Ba_2Ti_2(acac)_4(OEt)_8$ are unstable to heating which can drive off the volatile $Ti(OEt)_4$ or $Ti(acac)_2(OEt)_2$ fragments respectively, leading to segregation of the metals.[100] These two precursors both allow formation of $BaTiO_3$ by solution hydrolysis, but the latter precursor also forms $BaTi_2O_5$ and BaO by-products - hinting at easier segregation of the metals in this complex. Segregation during hydrolytic (sol-gel) treatment is also a concern, for example, the M-Ti (M = Ni, Co, Mg)

precursors $M_2Ti_2(acac)_4(OEt)_8$ partially hydrolyse to give 2x $M_5TiO(acac)_6(OEt)_6$ + 8x $Ti(acac)(OEt)_3$ demonstrating immediate metal segregation at an early stage of hydrolysis.[112] In a further example, the precursor $CoAl_2(acac)_3(OAc)O^iPr_4$ successfully produces homogeneous spinel $CoAl_2O_4$ when thermalized in the solid state or by CVD, however, sol-gel hydrolytic methods lead instead to a mixed phase product.[76]

Excellent examples of the use of β-diketonate ligands are the complexes prepared by Dikarev and co-workers; $LiMn_2(thd)_5$ (thd = 2,2,6,6-tetramethyl-3,5-heptanedionate) and $[LiM(tbaoac)_3]_2$ (M = Co or Fe, tbaoac = tert-butyl acetoacetonate) which act as volatile and air-stable SSPs for phase pure $LiMn_2O_4$, $LiCoO_2$ or $LiFeO_2$ cathode materials for Li-ion batteries (**Fig. 8**).[21, 22, 108] $LiMn_2(thd)_5$ is shown to be stable in non-coordinating solvents and decomposed directly via thermolysis under O_2 at 600 °C. The choice of an asymmetric β-diketonate ligand in $[LiCo(tbaoac)_3]_2$ was found to prohibit polymerisation and allow solubility of the complex in both coordinating and non-coordinating solvents; thermolysis as low as 280 °C led to phase pure $LiCoO_2$.[21] The use of an SSP is particularly advantageous for building thin film batteries where nm to µm thick films are required. Recent progress has revealed the trimetallic SSP $LiMnCo(thd)_5$, whose trimetallic structure can be confirmed in the gas phase by Direct Analysis in Real Time (DART) mass spectrometry, and can be used to make $LiMnCoO_4$.[113] The Dikarev group have also recently turned their attention to Na analogues, $[NaM(tbaoac)_3]_2$, of these SSPs, targeting cathodes for Na-ion battery technologies.[114]

Oxalate anions, $[C_2O_4]^{2-}$, have been used to form many 2D or 3D coordination networks which may incorporate secondary metals as counterions, e.g. $[Co(bipy)_3][Mn_2(C_2O_4)_3]\cdot H_2O$ (bipy=2,2'-bipyridine), these show promise to thermally decompose into CMOs, e.g. $CoMn_2O_4$, with facile ligand decomposition into CO_2 or CO.[86]

Using a bifunctional carboxylate/oxime ligand (POBC), which preferentially binds different metal fragments at each site, has been used to make Ti-Zn SSPs ($\{Zn(POBC)_2Ti(O^iPr)_3\}_2$) (**Fig. 9**) used in the preparation of $TiZnO_3$.[46] In this example the oxime coordinated titanium centre retains reactive alkoxide ligands whist the Zn is stabilised entirely by carboxylates. Therefore, upon reaction with moisture (from air) the Ti site undergoes hydrolysis, and condenses to build titanium oxide nanoparticles, which are surrounded by organic ligands containing encapsulated Zn atoms. Heating then allows decomposition of the remaining organic components and diffusion of Zn atoms into the oxide phase. The final product displayed greater homogeneity and a higher surface area in comparison to a control reaction using multi-source precursors.[46]

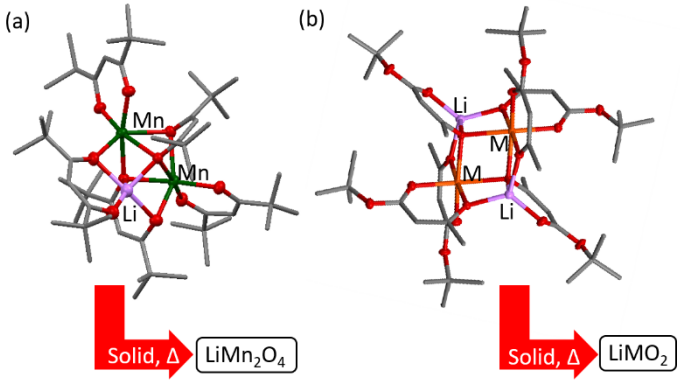

Fig. 8 Solid-state structures of heterometallic SSPs (a) $LiMn_2(thd)_5$ and (b) $[LiM(tbaoac)_3]_2$ (M = Co or Fe) and their decomposition products.

3.4 Oxo-bridged mixed-metal clusters with organic ligands

Mixed-metal alkoxides are susceptible to hydrolysis and condensation in the presence of small quantities of water, leading to a variety of further structures, including mixed-metal oxo-alkoxides, which may themselves act as suitable SSPs for CMO formation.[17] The introduction of oxo ligands may dramatically change the solubility of alkoxide precursors, especially if a polymeric alkoxide (typically insoluble) is converted into a molecular oxo-alkoxide cluster.[52, 100, 101]

Doped-polyoxotitanium cages (POTs) are an example of these oxo bridged species and arise from the partial hydrolysis and condensation of titanium alkoxides in the presence of a dopant metal source (e.g. metal chlorides). Solvothermal synthetic strategies can access metal doped POTs (M-POTs) of various compositions and sizes, and a series of M-POTs with formula $[Ti_xO_y(OR)_zM_nX_m]$ (M = main group element, transition metal or lanthanide metal; X = anion) has been developed.[49, 51] For some metal species, the stoichiometry of M and Ti can be tuned by changing the ratios of starting materials MX_w and $Ti(OR)_4$ (e.g. M = Co^{II}, Fe^{II}).[115] In other cases (e.g. M = Ce^{III}), multiple products, with differing M:Ti ratios, are formed from the reaction, but can be separated by fractional crystallisation.[41, 116]

The alkoxide-groups surrounding the Ti_xO_y cores of M-POT alkoxide cages are easy to hydrolyse, facilitating the deposition and further calcination of M-POTs at low temperatures. Low temperature hydrolysis and condensation may lead to the formation of the anatase phase of TiO_2 rather than the thermodynamically favoured rutile phase.[49, 51] As M-POTs are soluble in organic solvents, deposition of metal-doped TiO_2 on substrates can be easily realised using solution methods. Low temperature hydrolysis of a concentrated solution of $[Ti_{17}O_{28}(O^iPr)_{16}\{Co(phen)\}_2]$ (phen = phenanthroline), induced by moisture from the air, has been shown to generate hollow nanospheres of TiO_2 decorated with residual

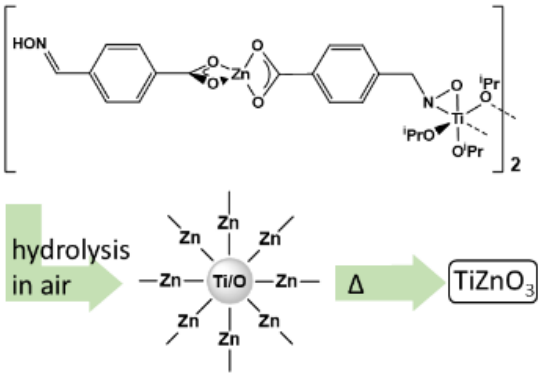

Fig. 9 Hydrolysis of a Ti-Zn SSP assembled using a bifunctional ligand. After hydrolysis Ti/O nanostructures, which are covered in Zn containing ligands, are converted to $TiZnO_3$ at >400°C.

Co(phenanthroline) fragments.[117] Using M-POT precursors can allow for a homogeneous distribution of the dopant metal ions in the TiO_2 products. For example, both energy-dispersive X-ray spectroscopy (EDS) and X-ray photoelectron spectroscopy (XPS) confirmed that sonication of Ce doped POTs (either $[Ti_{28}O_{38}(OEt)_{38}(EtOH)_{1.4}CeCl]$ (**Fig.10a**) or $[Ti_8O_7(OEt)_{21}(EtOH)Ce]$ (**Fig.10b**)) in 50 v% aqueous ethanol followed by calcination at 150 °C in air led to Ce^{III}-doped TiO_2 (either amorphous or anatase), with a Ce:Ti ratio matching that of the corresponding precursors (either 1:28 or 1:8). Surprisingly, after the same treatment for $[\{Ti_2O(OEt)_8\}(EtOH{\cdot}CeCl)]_2$ (**Fig.10c**), TiO_2 was obtained along with $Ce_2Ti_2O_7$ – an oxide that has only previously been made by solid-state techniques at high temperature (*ca.* 1000 °C).[118] Importantly, it is shown that the presence of TiO_2 in this mixed-phase product significantly stabilises the $Ce^{III}_2Ti_2O_7$, which otherwise will rapidly decompose to Ce^{IV} products at room-temperature in air.[41]

M-POTs have also acted as useful precursors for multifunctional composite CMOs, For example, after spin-coating $[Ti_2(OEt)_9(NiCl)]_2$ (**Fig.10d**) or $[Ti_4O(OEt)_{15}(CoCl)]$ (**Fig.10e**) onto photoelectrodes of p-Si, nano WO_3 or $BiVO_4$, the precursors hydrolysed (under air at room temperature) into composites of amorphous TiO_2 with NiO_x or $CoO/Co(OH)_2$. The amorphous TiO_2 acts as a protective layer, and the Co or Ni oxide species introduce catalytically active sites for water oxidation at the electrodes. Significantly improved activity and photostability of the composite photoelectrodes was found compared to those prepared without the deposition of Ti/M precursors.[119]

The formation of μ-oxo ligands can also be promoted by thermolysis of simple alkoxides, in turn forming new mixed-metal molecules which can be useful SSPs. For example, whilst sol-gel/annealing treatment of $Mg[Al(O^iPr)_4]_2$ leads to phase separation and formation of MgO and Al_2O_3 by-products, controlled thermolysis of the precursor can form $[MgAl_2(\mu_3\text{-}O)(O^iPr)_6]_4$ which acts as a far better SSP for formation of pure phase nanocrystalline spinel $MgAl_2O_4$ after sol-gel hydrolysis and annealing at only 475 °C.[23] It seems that a degree of pre-assembly in the oxo bridged precursor is beneficial for initiating formation of the (tertiary) spinel without binary oxide impurities.

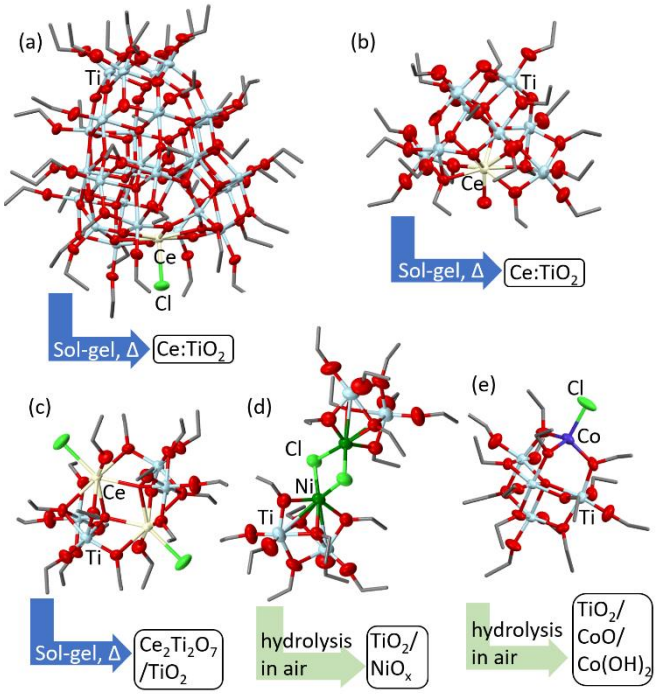

Fig. 10 Solid state structures of heterometallic SSPs (a) $[Ti_{28}O_{38}(OEt)_{38}(EtOH)_{1.4}CeCl]$, (b) $[Ti_8O_7(OEt)_{21}(EtOH)Ce]$, (c) $[\{Ti_2O(OEt)_8\}(EtOH{\cdot}CeCl)]_2$, (d) $[Ti_2(OEt)_9(NiCl)]_2$, (e) $[Ti_4O(OEt)_{15}(CoCl)]$ and their decomposition products.

3.5 Mixed-metal complexes with multidentate ligands

Multidentate ligands, including examples shown in **Fig. 11a**, such as salicylate (sal^{2-}=$OC_6H_4CO_2^{2-}$) or aminopolycarboxylates (such as ethylenediaminetetraacetate, $edta^{4-}$), can aid complexation of metals with high coordination numbers, such as heavy main group metals, e.g. Ba or Bi, as well as transition metals,[48] and allow for the formation of heterobimetallic complexes.[13, 55, 87, 120] Examples include $BaCo(cdta){\cdot}5H_2O$ (**Fig. 11b**),[60] $Bi_2Ti_3(sal)_8(Hsal)_2$ (**Fig. 11c**),[29] $[\{VO(bpy)(H_2O)\}_2\{Bi(edta)\}_4]{\cdot}30H_2O$ (bpy=2,2'-bipyridine) (**Fig. 11d**),[55] and $[M(H_2O)_5]_2[Ti_2(O_2)_2O(nta)_2]{\cdot}7H_2O$ (M = Co, Ni and Zn) (**Fig. 11e**).[13] Lewis acidic metals such as Bi may allow formation of a wide range of adduct complexes such as $Bi(Hsal)_6{\cdot}M(acac)_3$ (M= Al, Co, V, Fe, Cr) (**Fig. 11f**).[121] A series of Bi containing CMOs with high ionic conductivities and/or useful in photocatalytic applications, such as $Bi_2Al_4O_9$,[121] $Bi_4V_2O_{11}$,[55] and $BiMO_4$ (M=V, Nb, Ta),[59, 122] have been prepared using this type of SSP. It is important to note that these larger ligands lead to non-volatile species which precludes their use in CVD techniques, and their thermolysis may require longer heating times.[83]

Studies of these mulitdentate ligated SSPs have revealed the importance of temperature control and carbon content during annealing into an oxide phase. The Bi-Cu SSP $([Cu(H_2O)_2\{Bi(cdta)(H_2O)\}_2]{\cdot}H_2O)_n$ ($cdta^{4-}$= 1,2-cyclohexanediaminetetraacetate) will form pure-phase Bi_2CuO_4 at only 340 °C at a ramping rate of 0.2 °C·min^{-1}, however, on speeding up the heating process to 10 °C·min^{-1}, this phase only forms above 650 °C.[55] The related complex $[VO(H_2O)_3\{Bi(cdta)\}_2]{\cdot}7.7H_2O$ transforms to pure-phase $Bi_4V_2O_{11}$ when heated slowly to 630 °C at a rate of 0.2 °C·min^{-1}, however, when ramped more quickly at a rate of 10 °C·min^{-1}, a mixture of different oxides is obtained.[55] Whitmire and co-workers have shown that in this and related Bi_2-V SSPs a carbon content of ~30% is ideal for $Bi_4V_2O_{11}$ formation.[55] Similar results have been reported by Mentré and co-workers where a 31-32% carbon content in $cdta^{4-}$ ligated SSPs was successful for the formation of pure phase $BaCoO_{3-x}$,[60] whereas other related SSPs with different ligands led to mixed phases.

Another useful multidentate ligand system is singly deprotonated 'dipyridyldiol' ($[Py_2C(OH)O]^-$, see Fig. 11), which has been used by Driess and co-workers to build mixed-metal complexes which contain a central heterocubane $M_{4-x}M'_xO_4$ structure at their core.[30, 43, 44, 105] The ratio of M and M' in the cores can be adjusted by altering the ratio of starting materials, and since no exchange of metals is observed after synthesis, the initial mixture can be purified by chromatography to generate a cationic SSP of defined formula, e.g. $[Zn_3Ni\{Py_2C(OH)O\}_4]^{4+}$.[30]

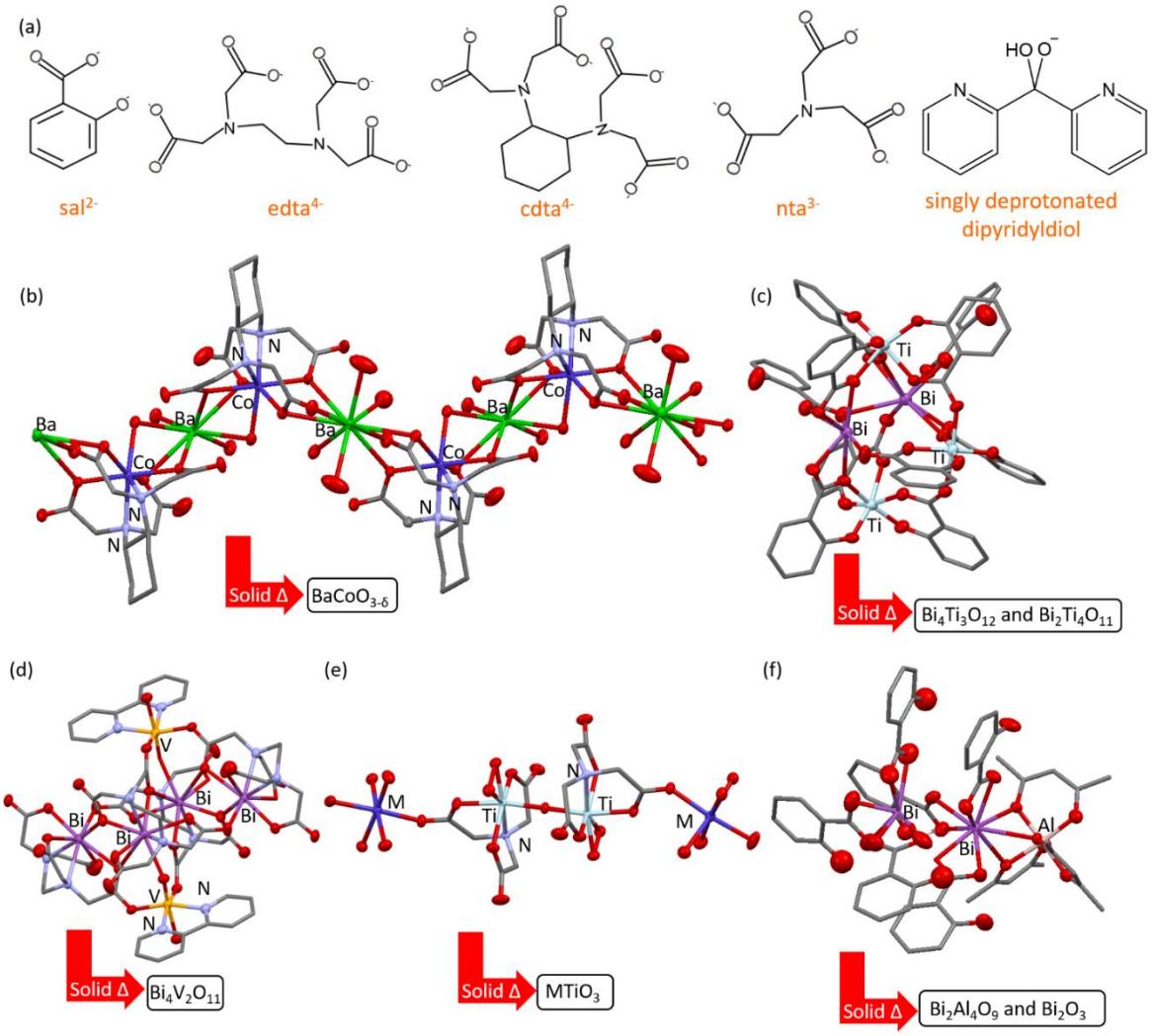

Fig. 11 Solid state structures of (a) common multidentate ligands, (b) BaCo(cdta)·5H_2O, (c) $Bi_2Ti_3(sal)_8(Hsal)_2$, (d) $[\{VO(bpy)(H_2O)\}_2\{Bi(edta)\}_4]\cdot 30H_2O$, (e) $[M(H_2O)_5]_2[Ti_2(O_2)_2O(nta)_2]\cdot 7H_2O$ (M = Co, Ni and Zn) and (f) $Bi(Hsal)_6\cdot Al(acac)_3$, and decomposition products of (b)-(f).

This Zn_3-Ni SSP allows access to 10 nm particles of Ni doped ZnO by thermolysis at 250 °C. Access to Ni doped ZnO is particularly interesting as Zn^{2+} and Ni^{2+} prefer different coordination geometries (e.g. tetrahedral and octahedral respectively in their monometallic oxides) and demixing may be expected. Indeed, at higher thermolysis temperature, which causes the formation of larger particle sizes (~44 nm at 500 °C), the metals begin to segregate and a mixture of $Ni_{0.7}Zn_{0.3}O$ and ZnO forms. This is an excellent example of how unusual solid phases can be accessed at small nanoparticle sizes, accessible only by low temperature decomposition of preformed SSPs.

Care must be taken when metals are coordinated to ligands with differing bond affinities, as these may thermalize at different rates. This may be the case if different types of coordination mode are found within an SSP, For example, the Zn-Cr precursor $[MeZnOCH_2PhCr(CO)_3]_4$ has been shown to thermally decompose initially to ZnO before forming a mixture of ZnO and $ZnCr_2O_4$.[18] This process is attributed to an initial loss of the Me and CO ligands at low temperatures (105-300 °C) releasing Zn to form ZnO, followed by decomposition of the aryl groups which coordinate Cr at higher temperature (330 °C), which then allows formation of the $ZnCr_2O_4$ spinel (**Fig. 12**) (still at much lower temperature than conventional ceramic methods, which may require 900 °C).

3.6 Mixed-metal polyoxometallates (M-POMs)

Polyoxometallates are metal-oxo clusters built from the aggregation of various $[MO_x]^{n-}$ blocks, typically supported from further condensation by an anionic charge. Whilst the core structures of POMs are normally based on high oxidation state metals Mo, W, V and Nb, there are now many examples of multimetallic POMS (M-POMs) where a secondary metal is incorporated into the cluster structure or acts as a counterion.

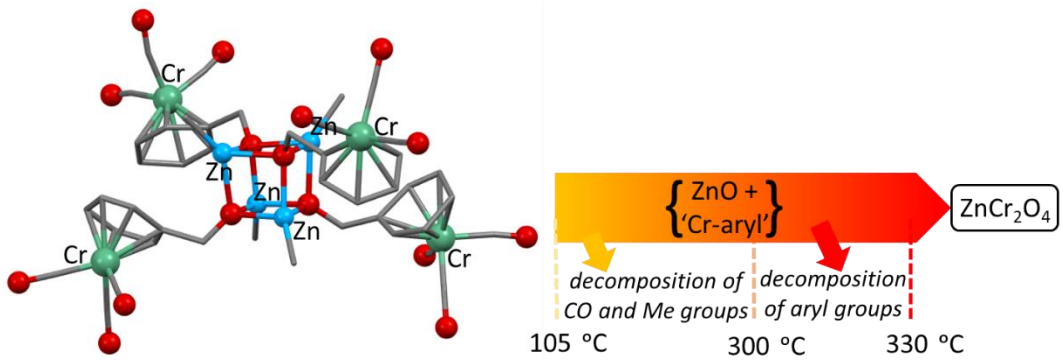

Fig. 12 Schematic illustration of the decomposition of $[MeZnOCH_2PhCr(CO)_3]_4$ SSP into $ZnCr_2O_4$.

These oxo clusters are well set up for decomposition into bulk oxide phases. $H_{4+x}[PMo_{11-x}V_{1+x}O_{40}]$ (x = 0, 3) and $[^nBu_4N]_{4+x}[PV_{1+x}W_{11-x}O_{40}]$ (x = 0, 1) have been used to make V-doped α-MoO_3 and WO_3 via AACVD at 550 °C.[53] Polyoxoniobate clusters have also been used to produce $LiNbO_3$ (**Fig. 13**),[35] and present a fascinating example of the importance of deposition and drying processes when forming (micro)crystalline films of SSPs prior to calcination. Nyman, Dolgos and co-workers examined the solution and drying behaviour of highly charged polyoxoniobate precursors $Li_8[Nb_6O_{19}]$ and $Li_6[H_2Nb_6O_{19}]$.[35] By exchanging two Li cations for two protons, they obtained $Li_6[H_2Nb_6O_{19}]$, an SSP with ideal stoichiometry for target oxide $LiNbO_3$, but this change also affected the charge of the anion and its agglomeration behaviour in aqueous solution (**Fig. 13**). Small angle X-ray scattering shows that the protonated precursor forms H-bonded dimers in solution, which dry upon spin coating into an amorphous glassy film. This can be calcined at 400 °C to form pure $LiNbO_3$. In contrast, the $Li_8[Nb_6O_{19}]$ SSP is more prone to agglomeration and crystallisation, leading to less even films upon drying, and it is found that alongside $LiNbO_3$ a perovskite impurity Li_3NbO_4 forms upon heating. The authors note the similar local structure within the perovskite to the polyoxoniobate cluster – suggesting that a greater degree of crystallisation of the molecular precursor before heating affects the oxide products. Furthermore, heating the mixture of $LiNbO_3/Li_3NbO_4$ at higher temperatures (600 °C) releases volatile Li_2O and forms Nb_2O_5.

It has recently been shown that polyoxovanadates (POVs) act as good precursors to access metal vanadates (MVO_4). Straightforward one-step routes have been developed to synthesise Bi-V SSP $[Bi_4(DMSO)_{12}V_{13}O_{40}]H_3$ and the series of M-POVs, $[Bi_2(DMSO)_6V_{12}O_{33}X]_2[M(DMSO)_6]$ (X = Cl, Br; M = Ca, Co, Ni, Cu, Zn) and $[Bi_2(DMSO)_6V_{12}O_{33}Cl]_2[Ln(DMSO)_6Cl]$ (Ln = La, Ce, Eu) using commercially available starting materials $VO(O^iPr)_3$, $Bi(NO_3)_3{\cdot}5H_2O$ and MCl_x.[26, 27] This synthetic route allows access to a wide range of metals occupying the role as counter cation, examples of rare and useful trimetallic SSPs. M-doped $BiVO_4$ photoanodes could then be prepared by drop-casting these precursors from DMSO solutions on to fluorine-doped tin oxide (FTO) substrates and annealing to 550 °C (**Fig. 14**). As these precursors are V rich, they act as type III SSPs with an amorphous V_2O_5 phase formed as a by-product alongside crystalline M-doped $BiVO_4$. The V_2O_5 (and any metal halides retained after decomposition) are removed by an alkaline washing step in most cases. EDS and XPS confirmed the formation of homogenous M-doped $BiVO_4$ (monoclinic Scheelite) when $M = Zn^{II}$, Ca^{II}, Ln^{III}, whilst composites of M:$BiVO_4$ with a minor secondary phase containing M-doped vanadium oxides occur when $M = Ni^{II}$, Co^{II}, and a mixture of doped and undoped $BiVO_4$ is found for $M = Cu^{II}$. $BiVO_4$ is a valuable material, well set up for photoelectrochemical water oxidation. In this case, the straightforward synthesis of a wide range of trimetallic SSPs allowed rapid screening of a series of M-dopants in $BiVO_4$. Compared to an undoped $BiVO_4$ photoanode similarly prepared from $[Bi_4(DMSO)_{12}V_{13}O_{40}]H_3$, all the

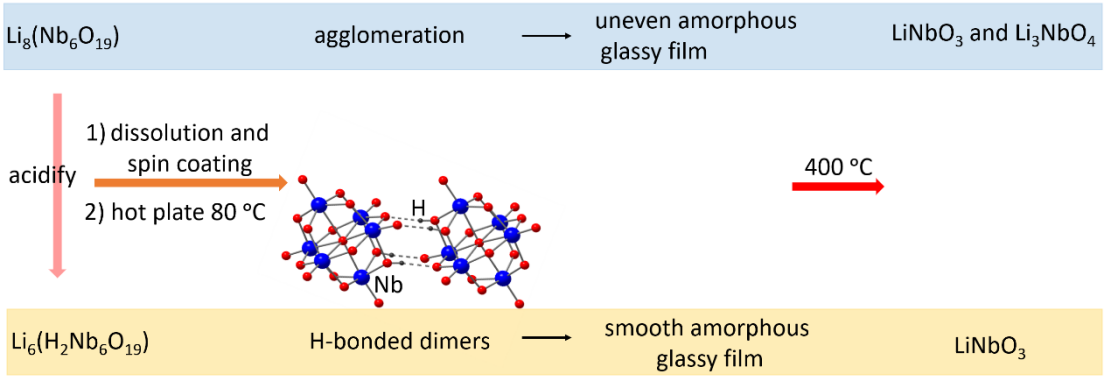

Fig. 13 Schematic illustration of the conversion of $Li_8(Nb_6O_{19})$ to $Li_6(H_2Nb_6O_{19})$ SSPs and their respective decomposition to complex metal oxides.

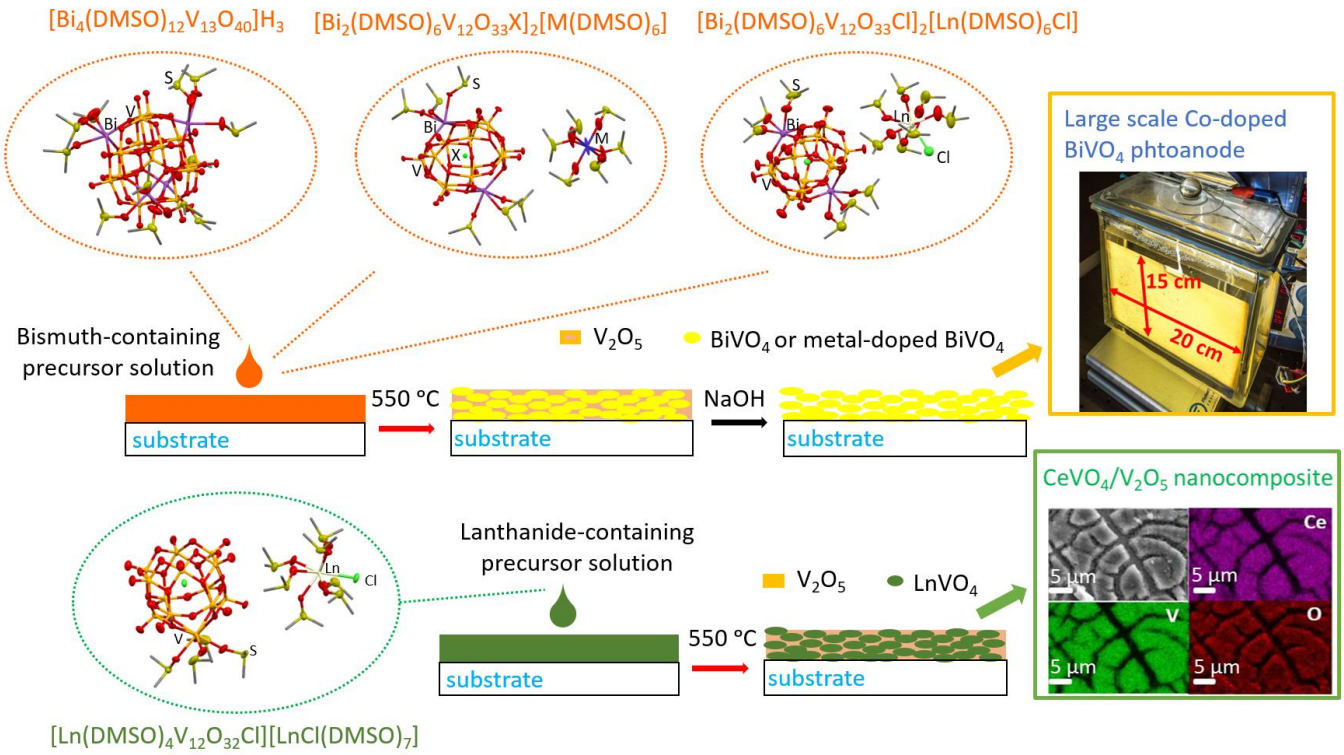

Fig. 14 Systematic illustration of using SSPs for preparation of metal doped-$BiVO_4$ and $LnVO_4/V_2O_5$ (Ln=Ce, Eu) nanocomposites.

transition metal doped $BiVO_4$ films showed improved photocatalytic activity (~1.8-2.4 times the photocurrent density of undoped $BiVO_4$ at 1.23 V *vs.* RHE) for solar water oxidation. In contrast, lanthanide or Ca-doping showed a detrimental effect. One intriguing aspect is that when Co-doped $BiVO_4$ was prepared, Co was observed to migrate to the surface of the photoanodes during use, where it is likely to act as a beneficial oxygen evolution catalyst - enhancing water oxidation efficiency. Therefore, in this example an SSP is used to directly build a complex functional material – $BiVO_4$ with a surface CoO_x layer. Using simple drop-casting techniques, Co-doped $BiVO_4$ photoanodes of up to 300 cm^2 could be prepared. Typically, large $BiVO_4$ photoanodes have only been prepared by more complicated or demanding routes (e. g. 35 cm^2 by sputtering techniques).[123] Therefore, using M-POVs as SSPs for the synthesis of $BiVO_4$ photoanodes may allow for the production of practically-sized devices for photoelectrochemical water splitting technologies. Another type of M-POV, $[Ln(DMSO)_4V_{12}O_{32}Cl][LnCl(DMSO)_7]$, was also shown to produce nanocomposites of $LnVO_4/V_2O_5$ (Ln=Ce, Eu) after thermal decomposition (without washing) (**Fig. 14**).[26, 27]

In recent years, many M-POV structures have been reported, many of these are yet untested as SSPs. For example, could $[Sr(DMF)_{2.5}(CON_2H_4)_2]_2[H_2V_{10}O_{28}]$ (DMF=dimethylformamide) and $(n\text{-}Bu_4N)_4[Cu_6V_{30}O_{82}(NO_3)_2(CH_3CN)_6]$,[124, 125] access MV_2O_6 (M = Sr, Cu) materials useful as sensors, photocatalysts and photoanodes?[126, 127]

3.7 Mixed-metal metal-organic frameworks

Metal-organic frameworks (MOFs) consist of organic linkers which extend infinitely in a periodic manner through metal based nodes to form 1D, 2D, or 3D structures.[128] MOFs often have tuneable porous structures, multiple topologies, and large surface areas. Mixed-metal MOFs can be fabricated by one-pot reactions or post-synthetic modification, which have been well discussed in a recent review.[129] In general, direct one-pot reactions tend to give mixed-metal MOFs with more clearly defined inter-metal ratios and/or heterometals occupying different sites, whilst post-synthetic modification may lack stoichiometric control.[129]

Many precisely structured mixed-metal MOFs have been used as SSPs for the synthesis of micro-/nano-scale metal oxides, e.g. $ZnMn_2$-ptcda (ptcda = perylene-3,4,9,10-tetracarboxylic dianhydride) can be used to form $ZnMn_2O_4$ nanoplates for use as battery anodes.[130] The as-prepared CMOs can retain the macroscopic particle shape of the parent MOF particles, and may thus possess higher surface areas and more desirable porous architectures compared to metal oxides produced by other methods.[24, 131, 132] This is especially useful for applications in which stable porous architectures are required, such as supercapacitors.[131, 133] Although many studies have reported the synthesis of CMOs by decomposition of mixed-metal MOFs,[131, 132, 134] the effects of metal distribution in the mixed-metal MOFs on the final CMOs have not been clearly revealed, probably due to the high complexity of the decomposition process.

Variations in annealing temperature and time can provide useful control over the composition, surface area, and pore size distribution of metal oxides derived from mixed-metal MOFs.[132] For example, when annealing mixed-metal MOF JUC-155, which contains octahedrally coordinated Zn and tetrahedrally coordinated Co (**Fig. 15**), a reduction in heating temperature

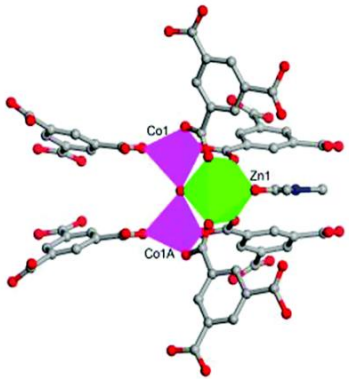

Fig. 15 Fundamental building unit of JUC-155, Reproduced from Ref. 58 with permission from the Royal Society of Chemistry.

from 500 °C to 400 °C, resulted in an increase of the surface area in the (pure-phase) $ZnCo_2O_4$ spinel product, useful as a supercapacitor.[58]

3.8 Statistically mixed precursors to CMOs

There are also many examples of statistically arranged mixed-metal compounds and frameworks falling in the categories discussed above. These 'imprecise' precursors are often straightforward to prepare and synthesis may favour mixed-metal rather than single-metal products for statistical reasons. These types of precursors enable mixing of metals at the molecular level and therefore carry many of the benefits of precisely defined SSPs. In a related scenario isostructural compounds with differing metal ratios often co-crystallise as a solid-solution such that the metals are essentially randomly mixed in the solid phase.[30]

An intriguing family of imprecise SSPs are $[M_{4-x}M'_x\{Py_2C(OH)O\}_4](OAc)_{4-y}(ClO_4)_y$ (M, M' = Zn, Mn, Ni, Co) synthesised by Driess and co-workers. As cationic species the various conformations can be identified by electrospray ionisation (ESI) mass spectrometry and any homometallic by-products may be removed by chromatography.[30, 43, 44] The mixed-metal Zn-Co SSPs decompose to different products compared to a mixture of the analogous homometallic Zn and Co precursors.[43] The compounds with a core of $[Zn_{4-x}Co_x\{Py_2C(OH)O\}_4]^{4+}$ (**Fig. 16a**) were solvolysed in benzylamine at low temperatures (180 °C) for 3 h to form homogenous Co-doped ZnO (Wurzite) without any impurities of spinel $ZnCo_2O_4$. EDS and high-resolution transmission electron microscopy confirmed that Co was incorporated within the ZnO lattice. In comparison, using a mixture of homometallic $[Zn_4\{Py_2C(OH)O\}_4]^{4+}$ and $[Co_4\{Py_2C(OH)O\}_4]^{4+}$ with the same total Co/Zn ratio under the same solvothermal process generated a mixture of CoO and Co:ZnO, indicating that Co doping can be improved by introducing the Co at the molecular level prior to oxide formation. When used as an electrochemical water oxidation catalyst, Co doped ZnO showed hundreds of times higher O_2 evolution rates than that of the CoO/Co:ZnO composite derived from multiple source precursors.[43] Similarly, Ni doped ZnO produced by analogous Zn-Ni precursors, transformed into a composite material after electrical activation that outperformed undoped NiO for water oxidation in terms of both stability and activity.[44]

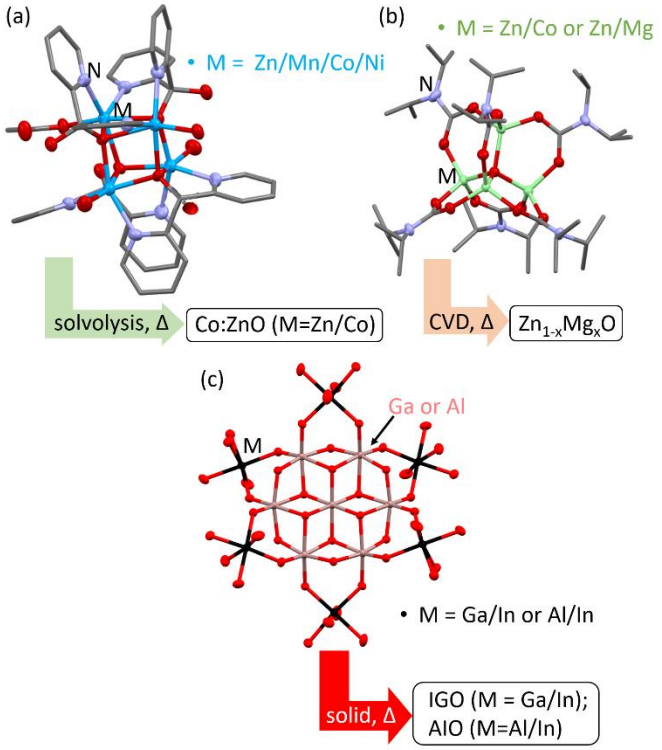

Fig. 16 Solid state structures and decomposition products of (a) $[M_{4-x}M'_x\{Py_2C(OH)O\}_4]^{4+}$ (M, M' = Zn, Mn, Ni, Co), (b) $Zn_{4-x}M_xO(O_2CNR_2)_6$ (M = Mg or Co), and (c) $[M_7In_6(\mu_3\text{-}OH)_6(\mu\text{-}OH)_{18}(H_2O)_{24}](NO_3)_{15}$ (M = Ga or Al).

The oxo clusters $Zn_{4-x}M_xO(O_2CNR_2)_6$ (M = Mg or Co) supported by carbamate ligands (**Fig. 16b**) are a further example of statistically mixed metals in a molecular precursor,[135, 136] with the differing stoichiometries identified by mass spectroscopy. The pre-mixed Zn/Mg SSPs are advantageous for producing a homogeneous $Zn_{1-x}Mg_xO$ material by CVD in comparison to using a mixture of homometallic precursors.[66]

Mixed-metal hydroxide 'flat' clusters have been prepared by Johnson and co-workers, with formula $[M_7In_6(\mu_3\text{-}OH)_6(\mu\text{-}OH)_{18}(H_2O)_{24}](NO_3)_{15}$ (M = Ga or Al) (**Fig. 16c**). These precursors have proven useful in the formation of the transparent conductors indium gallium oxide (IGO) and aluminium indium oxide (AIO) with approximate retention of the metal stoichiometry after calcination. The mixed-metal complexes can be prepared by several methods, but could be accessed by transmetallation reactions by adding $In(NO_3)_3$ to preformed monometallic Ga_{13} or Al_{13} clusters.[90] Isostructural clusters with lower indium content could also be prepared with formulae $[M_{(13-x)}M'_x(\mu_3\text{-}OH)_6(\mu\text{-}OH)_{18}(H_2O)_{24}](NO_3)_{15}$, where M = Ga or Al and M' = In, (x = 1-6). These have been shown to exist as statistical mixtures of each composition, each having different ^{1}H NMR spectroscopic signatures.[4, 90, 137]

Statistically mixed coordination polymers can also act as SSPs, for example, $LiM_xM'_yM''_z(acac)_3$ (M/M'/M'' = Ni, Mn, Co, x + y +

z = 1) with structures based on that of $LiCo(acac)_3$, allow access to a range of different Li-ion battery cathode materials $LiM_xM'_yM''_zO_2$ with varying metal contents.[138]

Imprecise mixed-metal MOFs may also act as useful precursors - for example MOF 74 may be prepared with Ni, Co or a mixture of the two metals. All variants display identical powder X-ray diffraction patterns and showed homogeneous distribution of metals by energy dispersive X-ray spectroscopic mapping. These MOFs can allow the formation of stoichiometrically controlled $Ni_xCo_{3-x}O_4$ species after calcination, with the mixed-MOFs forming only the mixed-metal spinel (and no formation of mono-metallic oxides).[25] This process is useful as the spinel $NiCo_2O_4$ may be used as a supercapacitor.

4. Looking beyond CMOs; mixed-metal SSPs for the synthesis of other complex materials

Whilst this article has focussed on the formation of complex metal oxides, SSP chemistry is not restricted to these materials and many other composite materials may be obtainable, for example $[Zn(TFA)_4Cu_3(dmae)_4]$ (dmae=N,N-dimethylaminoethanolate, TFA = trifluoroacetic acid) may be used to directly prepare Cu-ZnO composite materials by AACVD methods (**Fig. 17a**), such a combination of dispersed metallic nanoparticles on an oxide support is commonly used in heterogeneous catalysts.[139] In a recent example by Driess and co-workers, only carbonyl ligands were required to support a multimetallic cluster SSP, $Na_2[Rh_3Mn_3(CO)_{18}]$, which was used to prepare a Rh-MnO_x catalyst for the conversion of syngas to ethanol (**Fig. 17b**).[140] Mixed-metal sulphides may also be targeted, for instance using $[(Ph_3P)_2AgIn(SC\{O\}R)_4]$ (R = Me, Ph) can access $AgInS_2$ by direct thermolysis or $AgIn_5S_8$ films by AACVD (**Fig. 17c**).[141] Mixed-metal selenides are also obtainable from the related precursors $[(Ph_3P)_2MIn(SeC\{O\}R)_4]$ (M = Cu, Ag, R = Ph, tolyl)[142] or $[(Ph_3P)_2CuIn(SeCH_2CPh)_4]$.[143] Complex metal fluorides are also accessible, for example, coordination polymers $NaM(hfac)_4$ (M=Y, Eu, Gd or Er, hfac= hexafluoroacetylacetonate) can be decomposed to give $NaMF_4$ materials (with both kinetic and thermodynamic polymorphs accessible) (**Fig. 17d**),[144, 145] whilst the $[MM'(O_2CCF_3)_3]_n$ family (M = Mn with M' = Na, K, Rb and Cs; or M = Mg and Ca with M' = Rb; n=1 or 2) can allow access to $MMnF_3$ fluoroperovskites.[146-148]

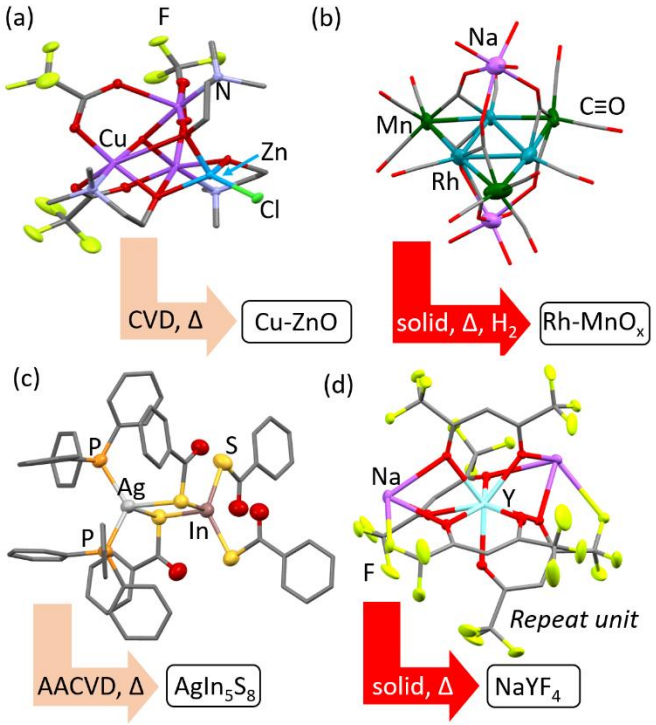

Fig. 17 Structures and decomposition products of (a) $[Zn(TFA)_4Cu_3(dmae)_4]$ and (b) $Na_2[Rh_3Mn_3(CO)_{18}]$ which form composite metal-metal oxide materials, (c) $[(Ph_3P)_2AgIn(SC\{O\}Ph)_4]$ which forms a mixed-metal sulphide, and (d) $NaY(hfac)_4$ which forms a mixed-metal fluoride product.

Table 1. Routes to CMOs using different groups of mixed metal SSPs (reported examples shown by ✓)

Mixed-metal SSP group	Solid State Thermolysis	Chemical Vapour Deposition	Hydrolytic Transformation	Solvolytic Transformation
General Comments	● *SSPs often allow access to CMOs at low temperatures and can access small particle sizes or unusual phases.* ● *Release of gases can increase porosity in product.* ● *Heat from combustion of organic components may aid low temperature crystallisation.* ● *During solution deposition of SSPs, the drying step, and crystallisation may influence the final product.*	● *Precursor must be volatile and stable in the gas phase.* ● *AACVD reduces requirements for volatility.* ● *Useful for producing high quality thin films* ● *Ligands with greater thermal stability may avoid unwanted organic polymerisation side reactions.*	● *Low temperature routes possible.* ● *SSPs ensure metals are pre-mixed at the molecular level at the beginning of the reaction, however, solution routes may allow rearrangement during hydrolysis.* ● *Slow hydrolysis can be conducted by simply exposing to air.*	● *Low temperature routes possible.* ● *Solvent or ligands supply oxygen atoms for CMO product.* ● *Solution rearrangements also possible.* ● *Slow reactivity favours crystalline products*
Alkoxides	✓ ● Compounds may be volatile or may thermally deconstruct to lose volatile fragments.	✓ ● May be thermally unstable, leading to metal segregation. ● Bulkier alkoxides or use of alkyls helps prevent oligomerisation and improves volatility.	✓ ● May be prone to metal segregation during solution hydrolysis.	✓ ● May be prone to metal segregation during solution reactions.
Complexes with oxygen donor ligands	✓ ● Bulky ligands may require longer heating times. ● Loss of volatile fragments possible. ● Different ligands (or binding sites of a bifunctional ligand) may decompose at different rates.	✓ ● May be thermally unstable, leading to metal segregation.	✓ ● May be prone to metal segregation during solution hydrolysis. ● Bifunctional ligands may help to retain close proximity of heterometals, even if hydrolysis proceeds at differing rates.	
Oxo-bridged clusters with organic ligands	✓ ● Different inter-metal ratios accessible.	✓ ● Smaller clusters can have good volatility.	✓ ● "Pre-assembly" of M-O-M bridges may improve product homogeneity. ● Different inter-metal ratios accessible.	
Complexes with multidentate ligands	✓ ● Carbon content and heating rate influential. ● Access to metals with high coordination numbers. ● Differing M-L bonding may decompose at different rates.	× ● Bulky ligands likely to lead to non-volatile compounds.		✓
M-POMs	✓ ● Deposition possible from aqueous solution. ● Anion-cation combinations to incorporate different metals.	✓ ● AACVD used.	× ● Stable molecular species in aqueous environments.	
Mixed-metal MOFs	✓ ● Access to products with high porosity.	× ● Non-volatile.	× ● Low solubility/ unreactive.	× ● Low solubility.

5. Summary and outlook

Using mixed-metal SSPs is a promising alternative strategy for synthesising a great variety of CMO materials. It is possible to control the stoichiometry, structure and homogeneity with a high degree of precision, which is often difficult when using a mixture of individual precursors. The synthesis of CMOs can often occur at much lower temperatures and over shorter timescales, owing to the pre-mixing of metals at the molecular level.[11, 23, 34, 41, 54, 56] Low temperature synthetic routes can allow access to new phases or those with high dopant content,[12, 30, 59] and to materials that have high porosity and/or small particles sizes.[30, 45, 58, 130] Examples demonstrate that synthesising CMOs from mixed-metal SSPs can improve their properties compared with those from mixtures of precursors.[43, 44, 46] Furthermore, many SSPs have good solubility, allowing for convenient processing and generating the potential for scale up of materials for practical applications using solution deposition techniques.[26, 27, 35, 49, 50, 51]

Whilst using SSPs may simplify synthetic routes to oxide materials, the synthesis of the SSPs themselves may be challenging, possibly requiring air-sensitive manipulation. In some ways, this shifts the synthetic challenges from the domain of materials chemists to that of synthetic inorganic chemists. A consideration of the cost, efficiency and difficulty of precursor synthesis, along with the stability of the SSP prior to use, is required when comparing SSPs with more readily available precursors. The influence of carbon content should be considered, as whilst organic combustion may aid low temperature crystallisation and increase porosity, too much carbon content can lead to carbon impurities. Furthermore, it is essential that users have a clear understanding of the precursor chemistry and the decomposition/reaction pathways to avoid the segregation of metals and loss of the carefully designed inter-metal ratio e.g. by unwanted reaction with donor solvents, thermal deconstruction, or rearrangements in solution caused by partial hydrolysis.[34, 35, 100, 101, 104, 112] In some cases these issues can be addressed by fine-tuning the ligands, for instance, to inhibit release of volatile organometallic fragments (e.g. by replacing methyl groups by bulkier phenyls).[104] One promising avenue for future study is the hydrolysis of SSPs in the solid-state by slow reaction with ambient air, as a means of retaining elemental homogeneity, due to the difficulty of demixing in the solid phase. This concept has already shown promise in the aerobic hydrolysis of M-POTs which generates amorphous TiO_2 decorated with heterometals.[49]

Reported applications of SSP derived materials include as photocatalysts,[26, 46, 89] (super)capacitors,[11, 12, 25, 34, 52, 58] transparent conductors[4, 42, 90, 102, 137] and as battery electrodes.[21, 22, 108, 114, 130, 138] With a good understanding of synthetic opportunities to mixed-metal complexes, current research is targeting specific high value oxides at the forefront of solid-state chemistry research and in real-world applications e.g. $BiVO_4$ (water oxidation),[26] $LiMO_2$[138] and $NaMO_2$ (lithium/sodium-ion battery cathodes).[114] Renewed interest in trimetallic SSPs is also present in current research.[26, 27, 99, 114] As highlighted in section 4, SSP chemistry is also diversifying to access many other mixed-metal materials other than oxides.

This area presents exciting future challenges in order to further our understanding of the transformation of molecules into materials. Factors, such as the effect of carbon content, the chemistry of molecular deposition/microcrystallisation, and the molecular structures of SSPs in the gas phase, are important for developing a rational understanding and predictability of the materials derived. Detailed mechanisms elucidating the transformation from a molecular precursor into a solid oxide remain rare but will contribute to understanding the formation of the final phase.[35] Future studies should report comparative studies that directly compare SSPs versus multi-source precursors,[11, 43, 44, 46, 149] as otherwise it can be challenging to evaluate the usefulness of a SSP method.

Many bi-, tri- and even tetra-metallic compounds are now known, with current uses in homogenous catalysis or as single molecular magnets, that have not been tested as SSPs - these could open up further opportunities for the convenient synthesis of CMOs and other functional materials.[150-152] With much recent interest in this area, mixed-metal compounds hold great promise for the synthesis of important CMOs for wider applications in chemistry and material science.

Conflicts of interest

There are no conflicts to declare.

Acknowledgements

We thank the following for financial support: the Herchel Smith Research Fund and the Royal Society University Research Fellowship (S. D. Pike).

References

1. X. Q. Liu, J. Iocozzia, Y. Wang, X. Cui, Y. H. Chen, S. Q. Zhao, Z. Li and Z. Q. Lin, *Energ. Environ. Sci.*, 2017, **10**, 402-434.
2. A. B. Djurisic, Y. H. Leung and A. M. C. Ng, *Mater. Horiz.*, 2014, **1**, 400-410.
3. C. Z. Ma, J. Alvarado, J. Xu, R. J. Clement, M. Kodur, W. Tong, C. P. Grey and Y. S. Meng, *J. Am. Chem. Soc.*, 2017, **139**, 4835-4845.
4. Z. L. Mensinger, J. T. Gatlin, S. T. Meyers, L. N. Zakharov, D. A. Keszler and D. W. Johnson, *Angew. Chem. Int. Edit.*, 2008, **47**, 9484-9486.
5. M. Mehring, *Coordin. Chem. Rev.*, 2007, **251**, 974-1006.
6. D. P. Dubal and P. Gomez-Romero, *Metal Oxides in Supercapacitors*, Elsevier, 2017.
7. W. M. Li, J. F. Zhao, L. P. Cao, Z. Hu, Q. Z. Huang, X. C. Wang, Y. Liu, G. Q. Zhao, J. Zhang, Q. Q. Liu, R. Z. Yu, Y. W. Long, H. Wu, H. J. Lin, C. T. Chen, Z. Li, Z. Z. Gong, Z. Guguchia, J. S. Kim, G. R. Stewart, Y. J. Uemura, S. Uchida and C. Q. Jin, *P. Natl. Acad. Sci.*, 2019, **116**, 12156-12160.
8. Q. L. Dai, M. E. Foley, C. J. Breshike, A. Lita and G. F. Strouse, *J. Am. Chem. Soc.*, 2011, **133**, 15475-15486.
9. J. Zhang, Z. Y. Qin, D. W. Zeng and C. S. Xie, *Phys. Chem. Chem. Phys.*, 2017, **19**, 6313-6329.

10. G. A. Seisenbaeva and V. G. Kessler, *Nanoscale*, 2014, **6**, 6229-6244.
11. M. Veith, *J. Chem. Soc., Dalton Trans.*, 2002, 2405-2412.
12. R. Petrus, A. Drag-Jarzabek, J. Utko, D. Bykowski, T. Lis and P. Sobota, *Inorg. Chem.*, 2017, **56**, 11365-11374.
13. Y. F. Deng, Q. Y. Lv, S. P. Wu and S. Z. Zhan, *Dalton Trans.*, 2010, **39**, 2497-2503.
14. P. Sobota, A. Drag-Jarzabek, L. John, J. Utko, L. B. Jerzykiewicz and M. Duczmal, *Inorg. Chem.*, 2009, **48**, 6584-6593.
15. S. Mathur, M. Veith, R. Rapalaviciute, H. Shen, G. F. Goya, W. L. Martins and T. S. Berquo, *Chem. Mater.*, 2004, **16**, 1906-1913.
16. A. A. Tahir, M. Mazhar, M. Hamid, K. G. U. Wijayantha and K. C. Molloy, *Dalton Trans.*, 2009, 3674-3680.
17. L. G. Hubert-Pfalzgraf, S. Daniele, R. Papiernik, M. C. Massiani, B. Septe, J. Vaissermann and J. C. Daran, *J. Mater. Chem.*, 1997, **7**, 753-762.
18. M. A. Dreher, M. Krumm, C. Lizandara-Pueyo and S. Polarz, *Dalton Trans.*, 2010, **39**, 2232-2238.
19. L. John, J. Utko, S. Szafert, L. B. Jerzykiewicz, L. Kepinski and P. Sobota, *Chem. Mater.*, 2008, **20**, 4231-4239.
20. S. Daniele, D. Tcheboukov and L. G. H. Pfalzgraf, *J. Mater. Chem.*, 2002, **12**, 2519-2524.
21. Z. Wei, H. X. Han, A. S. Filatov and E. V. Dikarev, *Chem. Sci.*, 2014, **5**, 813-818.
22. A. Navulla, L. Huynh, Z. Wei, A. S. Filatov and E. V. Dikarev, J. *Am. Chem. Soc.*, 2012, **134**, 5762-5765.
23. G. Mohammadnezhad, M. M. Amini and H. R. Khavasi, *Dalton Trans.*, 2010, **39**, 10830-10832.
24. Y. Y. Dong, Y. Wang, Y. N. Xu, C. C. Chen, Y. J. Wang, L. F. Jiao and H. T. Yuan, *Electrochim. Acta*, 2017, **225**, 39-46.
25. S. R. Chen, M. Xue, Y. Q. Li, Y. Pan, L. K. Zhu and S. L. Qiu, *J. Mater. Chem. A*, 2015, **3**, 20145-20152.
26. H. J. Lu, V. Andrei, K. J. Jenkinson, A. Regoutz, N. Li, C. E. Creissen, A. E. H. Wheatley, H. X. Hao, E. Reisner, D. S. Wright and S. D. Pike, *Adv. Mater.*, 2018, **30**, 1804033.
27. H. J. Lu, R. B. Jethwa, K. J. Jenkinson, A. E. H. Wheatley, H. X. Hao, D. S. Wright and S. D. Pike, *Dalton Trans.*, 2019, **48**, 4555-4564.
28. A. Drag-Jarzabek, R. Petrus and P. Sobota, *Inorg. Chem.*, 2016, **55**, 9524-9527.
29. J. H. Thurston and K. H. Whitmire, *Inorg. Chem.*, 2002, **41**, 4194-4205.
30. S. Polarz, A. V. Orlov, M. W. E. van den Berg and M. Driess, *Angew. Chem. Int. Edit.*, 2005, **44**, 7892-7896.
31. M. Niederberger, N. Pinna, J. Polleux and M. Antonietti, *Angew. Chem. Int. Edit.*, 2004, **43**, 2270-2273.
32. C. N. R. Rao, *Pure Appl. Chem.*, 1994, **66**, 1765-1772.
33. C. Y. Chang, H. I. Ho, T. Y. Hsieh, C. Y. Huang and Y. C. Wu, *Ceram. Int.*, 2013, **39**, 8245-8251.
34. B. C. Gaskins and J. J. Lannutti, *J. Mater. Res.*, 1996, **111**, 1953-1959.
35. Y. Hou, D. B. Fast, R. E. Ruther, J. M. Amador, L. B. Fullmer, S. R. Decker, L. N. Zakharov, M. R. Dolgos and M. Nyman, *J. Solid State Chem.*, 2015, **221**, 418-425.
36. U. Schubert, *J. Sol-Gel Sci. Techn.*, 2016, **79**, 249-261.
37. X. B. Huang, G. X. Zhao, G. Wang and J. T. S. Irvine, *Chem. Sci.*, 2018, **9**, 3623-3637.
38. S. Esposito, *Materials*, 2019, **12**, 668.
39. L. G. Hubert-Pfalzgraf, *J. Mater. Chem.*, 2004, **14**, 3113-3123.
40. C. Panda, P. W. Menezes and M. Driess, *Angew. Chem. Int. Edit.*, 2018, **57**, 11130-11139.
41. Y. K. Lv, M. M. Yao, J. P. Holgado, T. Roth, A. Steiner, L. H. Gan, R. M. Lambert and D. S. Wright, *RSC Adv.*, 2013, **3**, 13659-13662.
42. Y. Aksu and M. Driess, *Angew. Chem. Int. Edit.*, 2009, **48**, 7778-7782.
43. J. Pfrommer, M. Lublow, A. Azarpira, C. Gobel, M. Lucke, A. Steigert, M. Pogrzeba, P. W. Menezes, A. Fischer, T. Schedel-Niedrig and M. Driess, *Angew. Chem. Int. Edit.*, 2014, **53**, 5183-5187.
44. J. Pfrommer, A. Azarpira, A. Steigert, K. Olech, P. W. Menezes, R. F. Duarte, X. X. Liao, R. G. Wilks, M. Bar, T. Schedel-Niedrig and M. Driess, *Chemcatchem*, 2017, **9**, 672-676.
45. M. Veith, A. Altherr and H. Wolfanger, *Chem. Vap. Depos.*, 1999, **5**, 87-90.
46. J. X. Yang, J. Akbarzadeh, C. Maurer, H. Peterlik and U. Schubert, *J. Mater. Chem.*, 2012, **22**, 24034-24041.
47. M. Veith, S. Mathur, N. Lecerf, K. Bartz, M. Heintz and V. Huch, *Chem. Mater.*, 2000, **12**, 271-274.
48. M. Hamid, A. A. Tahir, M. Mazhar, M. Zeller and A. D. Hunter, *Inorg. Chem.*, 2007, **46**, 4120-4127.
49. P. D. Matthews, T. C. King and D. S. Wright, *Chem. Commun.*, 2014, **50**, 12815-12823.
50. K. Samedov, Y. Aksu and M. Driess, *Chem. Eur. J.*, 2012, **18**, 7766-7779.
51. M. Regue, K. Armstrong, D. Walsh, E. Richards, A. L. Johnson and S. Eslava, *Sustain. Energ. Fuels*, 2018, **2**, 2674-2686.
52. N. Y. T. Turova, E. P.; Kessler, V. G.; Yanovskaya, M. I., *J. Sol-Gel Sci. Techn.*, 1994, **2**, 17-23.
53. S. D. Ponja, S. Sathasivam, H. O. Davies, I. P. Parkin and C. J. Carmalt, *Chempluschem*, 2016, **81**, 307-314.
54. J. H. Boo, S. B. Lee, S. J. Ku, W. Koh, C. Kim, K. S. Yu and Y. Kim, *Appl. Surf. Sci.*, 2001, **169**, 581-586.
55. I. Bulimestru, S. Shova, N. Popa, P. Roussel, F. Capet, R. N. Vannier, N. Djelal, L. Burylo, J. P. Wignacourt, A. Gulea and K. H. Whitmire, *Chem. Mater.*, 2014, **26**, 6092-6103.
56. T. Ould-Ely, J. H. Thurston and K. H. Whitmire, *C. R. Chim.*, 2005, **8**, 1906-1921.
57. C. M. Lieberman, A. S. Filatov, Z. Wei, A. Y. Rogachev, A. M. Abakumov and E. V. Dikarev, *Chem. Sci.*, 2015, **6**, 2835-2842.
58. S. Chen, M. Xue, Y. Q. Li, Y. Pan, L. K. Zhu, D. L. Zhang, Q. R. Fang and S. L. Qiu, *Inorg. Chem. Front.*, 2015, **2**, 177-183.
59. J. H. Thurston and K. H. Whitmire, *Inorg. Chem.*, 2003, **42**, 2014-2023.
60. I. Bulimestru, O. Mentre, N. Tancret, A. Rolle, N. Djelal, L. Burylo, N. Cornei, N. Popa and A. Gulea, *J. Mater. Chem.*, 2010, **20**, 10724-10734.
61. H. T. Zhang, J. H. Yang, R. V. Shpanchenko, A. M. Abakumov, J. Hadermann, R. Clerac and E. V. Dikarev, *Inorg. Chem.*, 2009, **48**, 8480-8488.
62. S. Vallejos, D. F. Maggio, T. Shujah and C. Blackman, *Chemosensors*, 2016, **4**, 4010004.
63. P. Marchand, I. A. Hassan, I. P. Parkin and C. J. Carmalt, *Dalton Trans.*, 2013, **42**, 9406-9422.
64. L. G. Hubert-Pfalzgraf, *Inorg. Chem. Commun.*, 2003, **6**, 102-120.
65. P. Marchand and C. J. Carmalt, *Coordin. Chem. Rev.*, 2013, **257**, 3202-3221.

66. M. R. Hill, J. J. Russell and R. N. Lamb, *Chem. Mater.*, 2008, **20**, 2461-2467.
67. M. Andrieux, C. Gasqueres, C. Legros, I. Gallet, M. Herbst-Ghysel, M. Condat, V. G. Kessler, G. A. Seisenbaeva, O. Heintz and S. Poissonnet, *Appl. Surf. Sci.*, 2007, **253**, 9091-9098.
68. V. G. Kessler, G. A. Seisenbaeva and S. Gohil, *Surf. Coat. Tech.*, 2007, **201**, 9082-9088.
69. G. A. Seisenbaeva, S. Gohil, V. G. Kessler, M. Andrieux, C. Legros, P. Ribot, M. Brunet and E. Scheid, *Appl. Surf. Sci.*, 2011, **257**, 2281-2290.
70. N. Khan, A. Badshah, B. Lal, M. A. Malik, J. Raftery, P. O'Brien and A. A. Altaf, *Polyhedron*, 2014, **69**, 40-47.
71. M. A. Ehsan, H. Khaledi, A. Pandikumar, N. M. Huang, Z. Arifin and M. Mazhar, *J. Solid State Chem.*, 2015, **230**, 155-162.
72. K. G. Caulton and L. G. Hubertpfalzgraf, *Chem. Rev.*, 1990, **90**, 969-995.
73. V. G. Kessler, G. I. Spijksma, G. A. Seisenbaeva, S. Hakansson, D. H. A. Blank and H. J. M. Bouwmeester, *J. Sol-Gel Sci. Techn.*, 2006, **40**, 163-179.
74. M. Niederberger, *Acc. Chem. Res.*, 2007, **40**, 793-800.
75. G. A. Seisenbaeva, V. G. Kessler, R. Pazik and W. Strek, *Dalton Trans.*, 2008, 3412-3421.
76. G. A. Seisenbaeva, E. V. Suslova, M. Kritikos, V. G. Kessler, L. Rapenne, M. Andrieux, F. Chassagneux and S. Parola, *J. Mater. Chem.*, 2004, **14**, 3150-3157.
77. P. H. C. Camargo, G. G. Nunes, G. R. Friedermann, D. J. Evans, G. J. Leigh, G. Tremiliosi-Filho, E. L. de Sa, A. J. G. Zarbin and J. F. Soares, *Mater. Res. Bull.*, 2003, **38**, 1915-1928.
78. S. Mathur, M. Veith, M. Haas, A. Shen, N. Lecerf, V. Huch, S. Hufner, R. Haberkorn, H. P. Beck and M. Jilavi, *J. Am. Ceram. Soc.*, 2001, **84**, 1921-1928.
79. M. Niederberger and G. Garnweitner, *Chem. Eur. J.*, 2006, **12**, 7282-7302.
80. A. Vioux, *Chem. Mater.*, 1997, **9**, 2292-2299.
81. J. X. Yang, L. Lukashuk, J. Akbarzadeh, M. Stoger-Pollach, H. Peterlik, K. Fottinger, G. Rupprechter and U. Schubert, *Chem. Eur. J.*, 2015, **21**, 885-892.
82. J. A. Garden and S. D. Pike, *Dalton Trans.*, 2018, **47**, 3638-3662.
83. L. John and P. Sobota, *Acc. Chem. Res.*, 2014, **47**, 470-481.
84. L. John, M. Kosinska-Klahn, L. B. Jerzykiewicz, L. Kepinski and P. Sobota, *Inorg. Chem.*, 2012, **51**, 9820-9832.
85. L. Andros, M. Juric, J. Popovic and P. Planinic, *RSC Adv.*, 2014, **4**, 37051-37060.
86. J. Habjanic, M. Juric, J. Popovic, K. Molcanov and D. Pajic, *Inorg. Chem*., 2014, **53**, 9633-9643.
87. F. Gschwind, O. Sereda and K. M. Fromm, *Inorg. Chem.*, 2009, **48**, 10535-10547.
88. T. Groer and M. Scheer, *J. Chem. Soc., Dalton Trans.*, 2000, 647-653.
89. S. J. A. Moniz, R. Quesada-Cabrera, C. S. Blackman, J. W. Tang, P. Southern, P. M. Weaver and C. J. Carmalt, *J. Mater. Chem. A*, 2014, **2**, 2922-2927.
90. M. K. Kamunde-Deyonish, M. N. Jackson, Z. L. Mensinger, L. N. Zakharov and D. W. Johnson, *Inorg. Chem.*, 2014, **53**, 7101-7105.
91. A. Drag-Jarzabek, M. Kosinska, L. John, L. B. Jerzykiewicz and P. Sobota, *Chem. Mater.*, 2011, **23**, 4212-4219.
92. A. Drag-Jarzabek, L. John, R. Petrus, M. Kosinska-Klahn and P. Sobota, *Chem. Eur. J.*, 2016, **22**, 4780-4788.
93. N. Y. Turova, Turevskaya, E.P., Kessler, V.G., Yanovskaya, M.I. , *The chemistry of metal alkoxides*, Kluwer Academic Publisher, Boston, 2002.
94. G. G. Nunes, D. M. Reis, P. T. Amorim, E. L. Sa, A. S. Mangrich, D. J. Evans, P. B. Hitchcock, G. J. Leigh, F. S. Nunes and J. F. Soares, *New J. Chem.*, 2002, **26**, 519-522.
95. Y. K. Gun'ko, U. Cristmann and V. G. Kessler, *Eur. J. Inorg. Chem.*, 2002, **5**, 1029-1031.
96. V. G. Kessler, *Chem. Commun.*, 2003, 1213-1222.
97. M. Veith, S. Mathur and V. Huch, *Inorg. Chem.*, 1996, **35**, 7295-7303.
98. M. Veith, S. Mathur and C. Mathur, *Polyhedron*, 1998, **17**, 1005-1034.
99. T. Heidemann and S. Mathur, *Inorg. Chem.*, 2017, **56**, 234-240.
100. V. G. Kessler, L. G. Hubert-Pfalzgraf, S. Daniele and A. Gleizes, *Chem. Mater.*, 1994, **6**, 2336-2342.
101. L. G. Hubertpfalzgraf, *Polyhedron*, 1994, **13**, 1181-1195.
102. Y. Aksu, S. Frasca, U. Wollenberger, M. Driess and A. Thomas, *Chem. Mater.*, 2011, **23**, 1798-1804.
103. J. F. Eichler, O. Just and W. S. Rees, *J. Mater. Chem.*, 2004, **14**, 3139-3143.
104. M. Tsaroucha, Y. Aksu, J. D. Epping and M. Driess, *Chempluschem*, 2013, **78**, 62-69.
105. M. Tsaroucha, Y. Aksu, E. Irran and M. Driess, *Chem. Mater.*, 2011, **23**, 2428-2438.
106. P. S. Koroteev, Z. V. Dobrokhotova and V. M. Novotortsev, *Russ. J. Gen. Chem.*, 2018, **88**, 1290–1305.
107. C. M. Lieberman, A. Navulla, H. T. Zhang, A. S. Filatov and E. V. Dikarev, *Inorg. Chem.*, 2014, **53**, 4733-4738.
108. H. X. Han, Z. Wei, M. C. Barry, A. S. Filatov and E. V. Dikarev, *Dalton Trans.*, 2017, **46**, 5644-5649.
109. C. M. Lieberman, Z. Wei, A. S. Filatov and E. V. Dikarev, *Inorg. Chem.*, 2016, **55**, 3946-3951.
110. G. A. Seisenbaeva, S. Gohil and V. G. Kessler, *J. Mater. Chem.*, 2004, **14**, 3177-3190.
111. C. Gasquères, I. Gallet, M. Herbst-Ghysel, M. Andrieux, M. Condat, V. G. Kessler, G. A. Seisenbaeva and S. Poissonnet, presented in part at the 15th European Conference on Chemical Vapor Deposition, Bochum, 2005.
112. G. A. Seisenbaeva, T. Mallah and V. G. Kessler, *Dalton Trans.*, 2010, **39**, 7774-7779.
113. H. X. Han, Z. Wei, A. S. Filatov, J. C. Carozza, M. Alkan, A. Y. Rogachev, A. Shevtsov, A. M. Abakumov, C. Pak, M. Shatruk, Y. S. Chen and E. V. Dikarev, *Chem. Sci.*, 2019, **10**, 524-534.
114. H. X. Han, Z. Zhou, J. C. Carozza, J. Lengyel, Y. Yao, Z. Wei and E. V. Dikarev, *Chem. Commun.*, 2019, **55**, 7243-7246.
115. S. Eslava, M. McPartlin, R. I. Thomson, J. M. Rawson and D. S. Wright, *Inorg. Chem.*, 2010, **49**, 11532-11540.
116. Y. K. Lv, J. Willkomm, M. Leskes, A. Steiner, T. C. King, L. H. Gan, E. Reisner, P. T. Wood and D. S. Wright, *Chem. Eur. J.*, 2012, **18**, 11867-11870.
117. Y. Y. Wu, P. Wang, Y. H. Wang, J. B. Jiang, G. Q. Bian, Q. Y. Zhu and J. Dai, *J. Mater. Chem. A*, 2013, **1**, 9862-9868.
118. M. Martos, B. Julian-Lopez, J. V. Folgado, E. Cordoncillo and P. Escribano, *Eur. J. Inorg. Chem.*, 2008, **2008**, 3163-3171.
119. Y. H. Lai, D. W. Palm and E. Reisner, *Adv. Energy Mater.*, 2015, **5**, 1501668.

120. J. H. Thurston, A. Kumar, C. Hofmann and K. H. Whitmire, *Inorg. Chem.*, 2004, **43**, 8427-8436.
121. J. H. Thurston, D. Trahan, T. Ould-Ely and K. H. Whitmire, *Inorg. Chem.*, 2004, **43**, 3299-3305.
122. J. H. Thurston, T. Ould-Ely, D. Trahan and K. H. Whitmire, *Chem. Mater.*, 2003, **15**, 4407-4416.
123. L. Chen, F. M. Toma, J. K. Cooper, A. Lyon, Y. J. Lin, I. D. Sharp and J. W. Ager, *Chemsuschem*, 2015, **8**, 1066-1071.
124. J. Forster, B. Rosner, R. H. Fink, L. C. Nye, I. Ivanovic-Burmazovic, K. Kastner, J. Tucher and C. Streb, *Chem. Sci.*, 2013, **4**, 418-424.
125. B. Schwarz and C. Streb, *Dalton Trans.*, 2015, **44**, 4195-4199.
126. R. Karthik, J. V. Kumar, S. M. Chen, P. S. Kumar, V. Selvam and V. Muthuraj, *Sci. Rep.*, 2017, **7**, 7254.
127. I. Khan and A. Qurashi, *Sci. Rep.*, 2017, **7**, 14370.
128. L. F. Xamena and J. Gascon, *Metal Organic Frameworks as Heterogeneous Catalysts*, Royal Society of Chemistry, 2013.
129. S. Abednatanzi, P. G. Derakhshandeh, H. Depauw, F. X. Coudert, H. Vrielinck, P. Van Der Voort and K. Leus, *Chem. Soc. Rev.*, 2019, **48**, 2535-2565.
130. J. Zhao, F. Q. Wang, P. P. Su, M. R. Li, J. Chen, Q. H. Yang and C. Li, *J. Mater. Chem.*, 2012, **22**, 13328-13333.
131. Y. Li, Y. X. Xu, W. P. Yang, W. X. Shen, H. G. Xue and H. Pang, *Small*, 2018, **14**, 1704435.
132. R. R. Salunkhe, Y. V. Kaneti and Y. Yamauchi, *ACS Nano*, 2017, **11**, 5293-5308.
133. N. N. Adarsh, in *Metal Oxides in Supercapacitors*, eds. D. P. Dubal and P. Gomez-Romero, Elsevier, 2017, pp. 165-192.
134. S. R. Wu, J. B. Liu, H. Wang and H. Yan, *Int. J. Energy Res.*, 2019, **43**, 697-716.
135. A. J. Petrella, H. Deng, N. K. Roberts and R. N. Lamb, *Chem. Mater.*, 2002, **14**, 4339-4342.
136. D. Domide, O. Walter, S. Behrens, E. Kaifer and H. J. Himmel, *Eur. J. Inorg. Chem.*, 2011, 860-867.
137. A. F. Oliveri, L. A. Wills, C. R. Hazlett, M. E. Carnes, I. Y. Chang, P. H. Y. Cheong and D. W. Johnson, *Chem. Sci.*, 2015, **6**, 4071-4085.
138. M. F. Li, J. J. Liu, T. C. Liu, M. J. Zhang and F. Pan, *Chem. Commun.*, 2018, **54**, 1331-1334.
139. M. Shahid, M. Mazhar, M. Hamid, P. O'Brien, M. A. Malik, M. Helliwell and J. Raftery, *Dalton Trans.*, 2009, 5487-5494.
140. P. Preikschas, J. Bauer, X. Huang, S. L. Yao, R. N. d'Alnoncourt, R. Kraehnert, A. Trunschke, F. Rosowski and M. Driess, *Chemcatchem*, 2019, **11**, 885-892.
141. T. C. Deivaraj, J. H. Park, M. Afzaal, P. O'Brien and J. J. Vittal, *Chem. Commun.*, 2001, 2304-2305.
142. S. Ghoshal, L. B. Kumbhare, V. K. Jain and G. K. Dey, *B. Mater. Sci.*, 2007, **30**, 173-178.
143. M. K. Pal, S. Dey, S. Neogy and M. Kumar, *RSC Adv.*, 2019, **9**, 18302-18307.
144. M. C. Barry, Z. Wei, T. Y. He, A. S. Filatov and E. V. Dikarev, *J. Am. Chem. Soc.*, 2016, **138**, 8883-8887.
145. S. Battiato, P. Rossi, P. Paoli and G. Malandrino, *Inorg. Chem.*, 2018, **57**, 15035-15039.
146. B. D. Dhanapala, H. N. Munasinghe, L. Suescun and F. A. Rabuffeti, *Inorg. Chem.*, 2017, **56**, 13311-13320.
147. E. Sathiyaraj, S. Thirumaran, S. Ciattini and S. Selvanayagam, *Inorganica Chim. Acta*, 2019, **498**, 119162.
148. R. G. Szlag, L. Suescun, B. D. Dhanapala and F. A. Rabuffetti, *Inorg. Chem.*, 2019, **58**, 3041-3049.
149. C. Limberg, M. Hunger, W. Habicht and E. Kaifer, *Inorg. Chem.*, 2002, **41**, 3359-3365.
150. N. Bridonneau, L. M. Chamoreau, P. P. Laine, W. Wernsdorfer and V. Marvaud, *Chem. Commun.*, 2013, **49**, 9476-9478.
151. T. Minato, K. Suzuki, Y. Ohata, K. Yamaguchi and N. Mizuno, *Chem. Commun.*, 2017, **53**, 7533-7536.
152. M. Liberka, J. Kobylarczyk, T. M. Muziol, S. Ohkoshi, S. Chorazy and R. Podgajny, *Inorg. Chem. Front.*, 2019, **6**, 3104-3118.